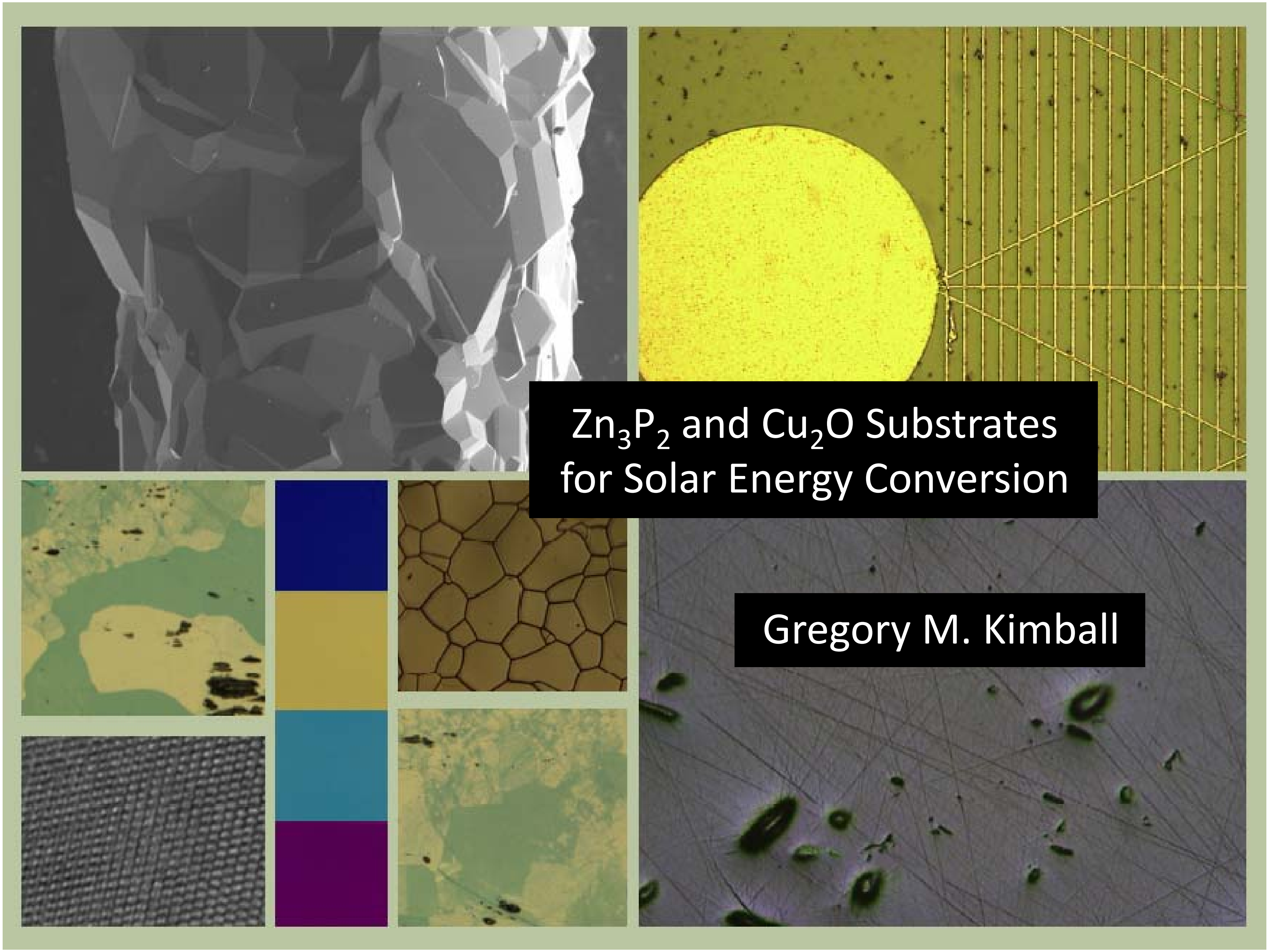
Zn_3P_2 and Cu_2O Substrates
for Solar Energy Conversion
Gregory M. Kimball

Photovoltaics market: 1990 – present

Photovoltaics market composition

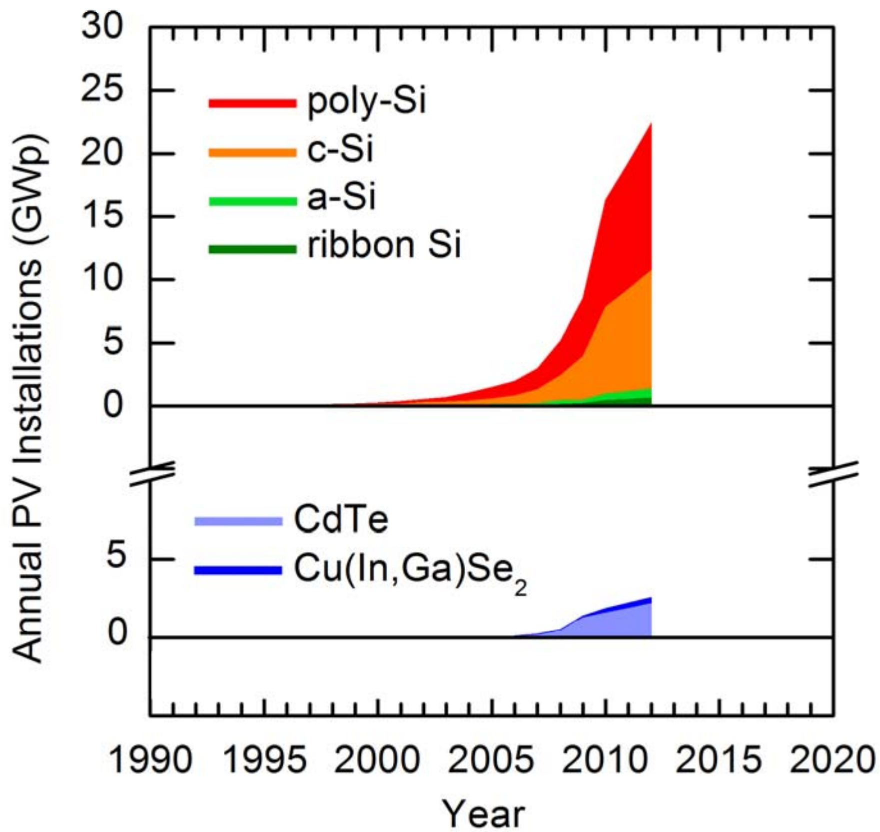

- What should we make our solar cells out of?
- How can we make installing PV cost less than laying concrete?

➢ **The future is wide open for new ideas!**

"Price, technology and the illusion of control." Paula Mints, Navigant Consulting. 21 April 2011.
"Global PV market, 2011." Chihheng Liang, Digitimes Research, Taipei. 11 May 2011.

Earth-abundant thin films

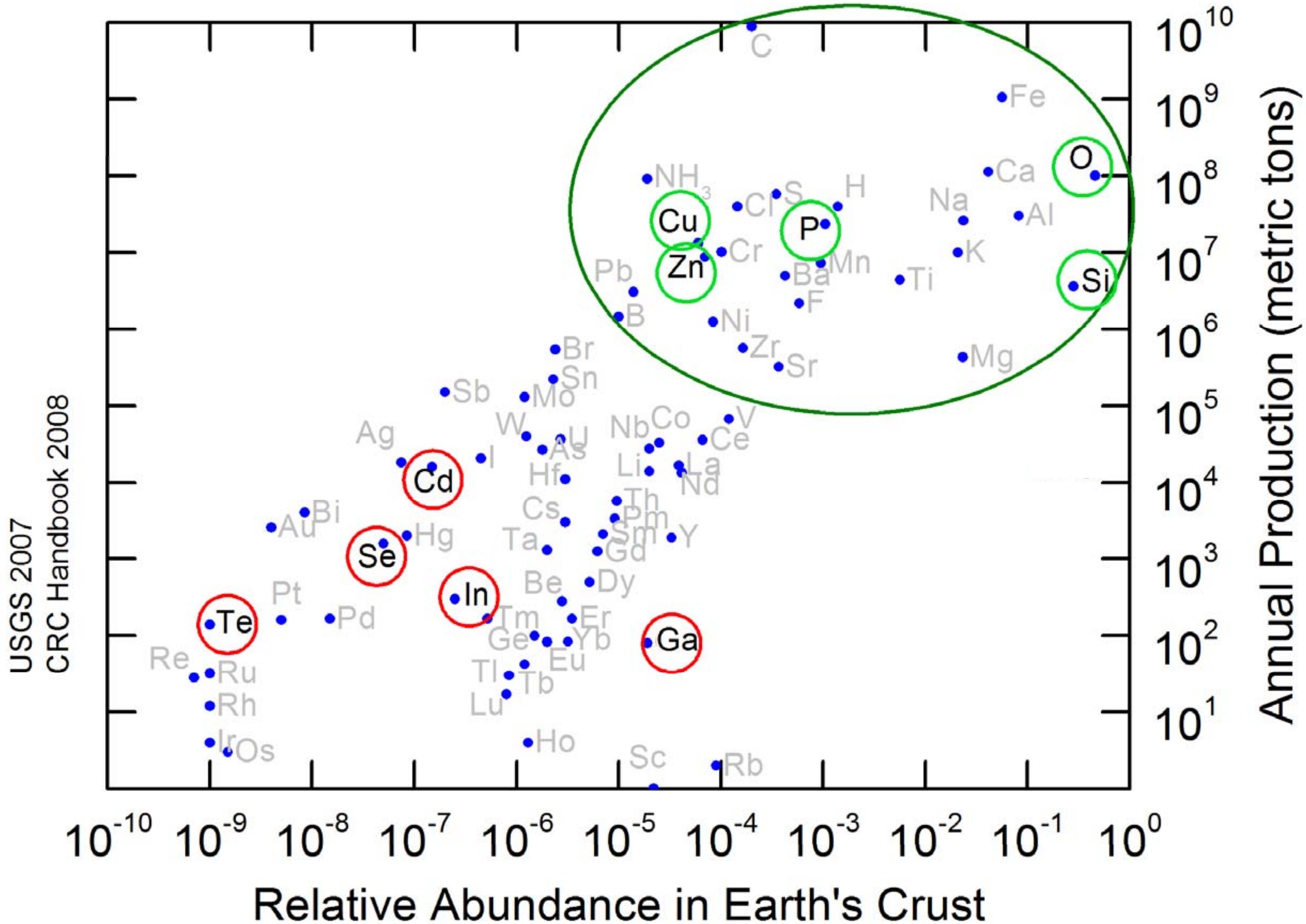

Zn_3P_2 and Cu_2O substrates for solar energy conversion

Cornering the market for 'Solar-Grade' Zn_3P_2

Why is annealing critical in Mg/Zn_3P_2 solar cells?

High performance Cu_2O/liquid junctions

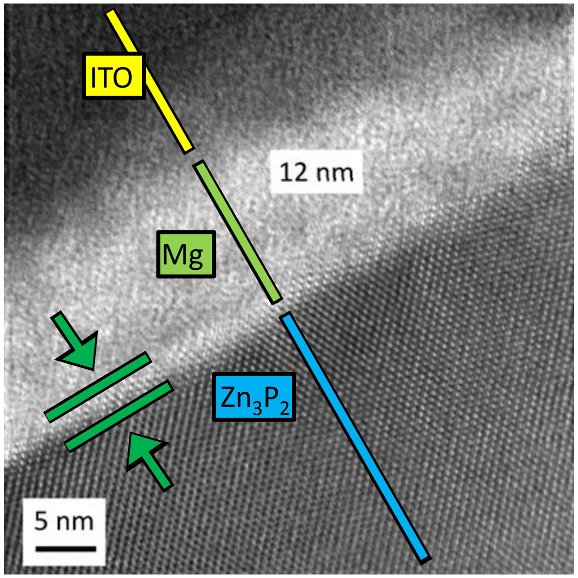

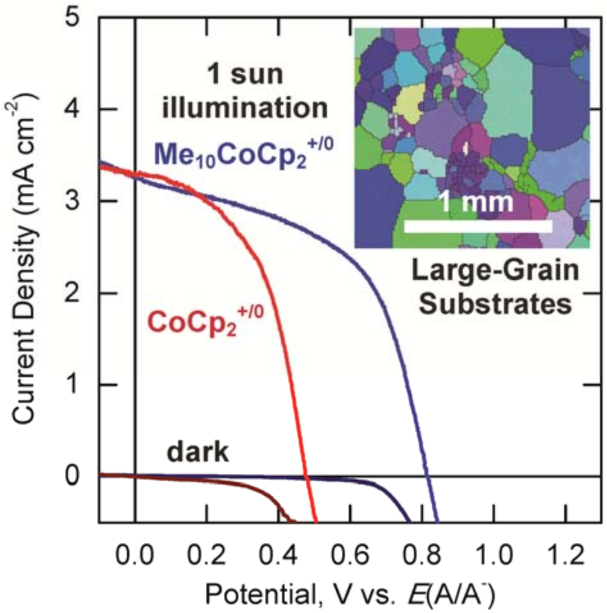

Zn_3P_2 and Cu_2O substrates for solar energy conversion

Cornering the market for 'Solar-Grade' Zn_3P_2

Why is annealing critical in Mg/Zn_3P_2 solar cells?

High performance Cu_2O/liquid junctions

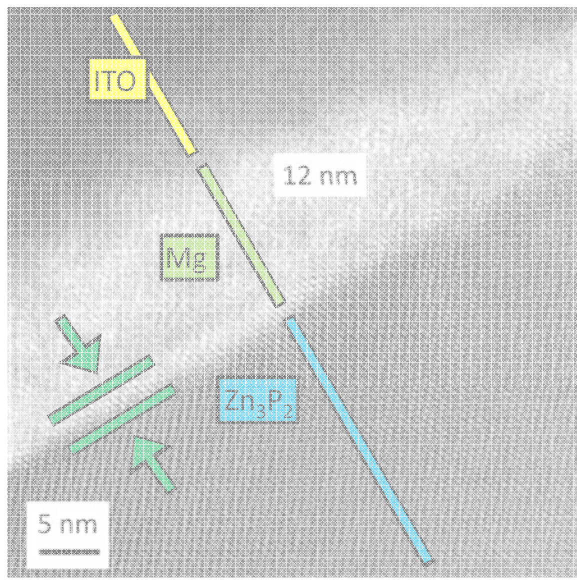

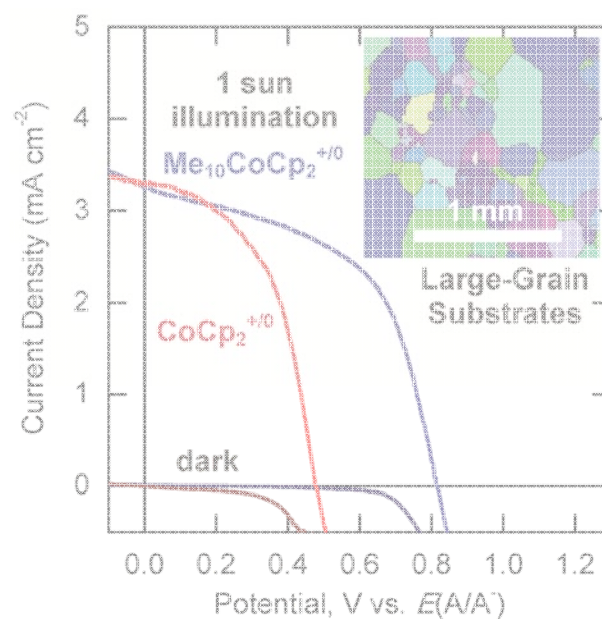

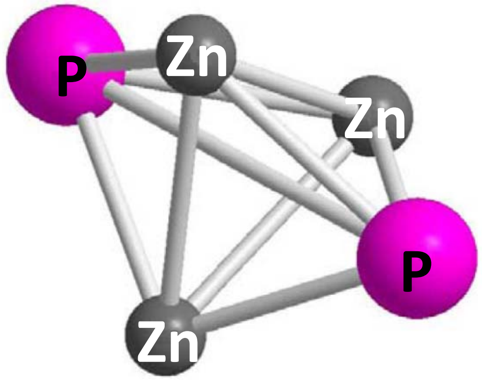

Zn_3P_2 for rodenticide

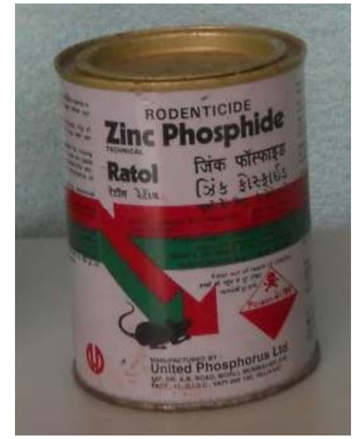

- Readily synthesized from zinc and phosphorus
- Selective for rodents, environmentally safe
- Market size: 100's of tons, 1000's of km^2 cropland
- Keeps rats off your roof!

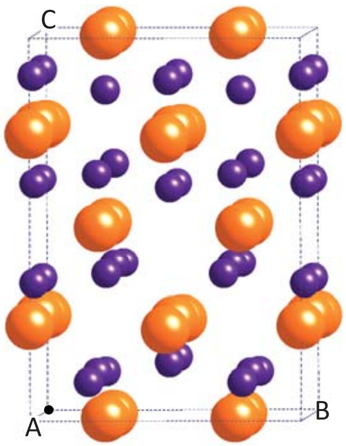

Zn_3P_2 for photovoltaics

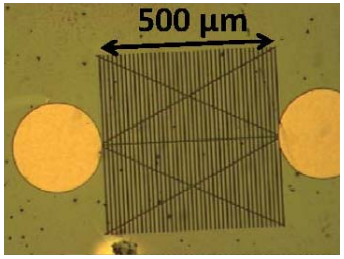

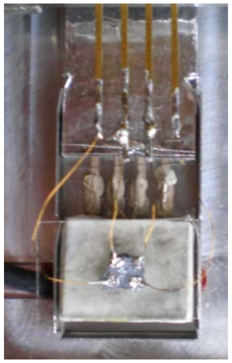

- Readily synthesized from zinc and phosphorus
- Direct 1.5 eV band gap, environmentally safe
- Mg/Zn_3P_2 solar cells of 6% efficiency
- Keeps rats off your roof!

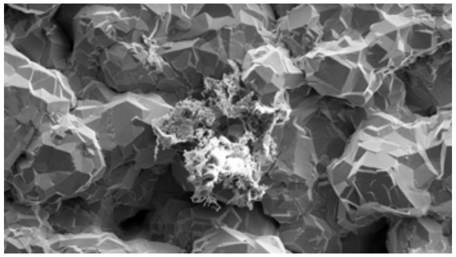

Zn_3P_2 from the elements

- High purity 99.9999% red phosphorus and zinc shot
- High temperature reaction in vacuum-sealed quartz tubes

➢ **Quantitative yield of 99.999+% Zn_3P_2 powders**

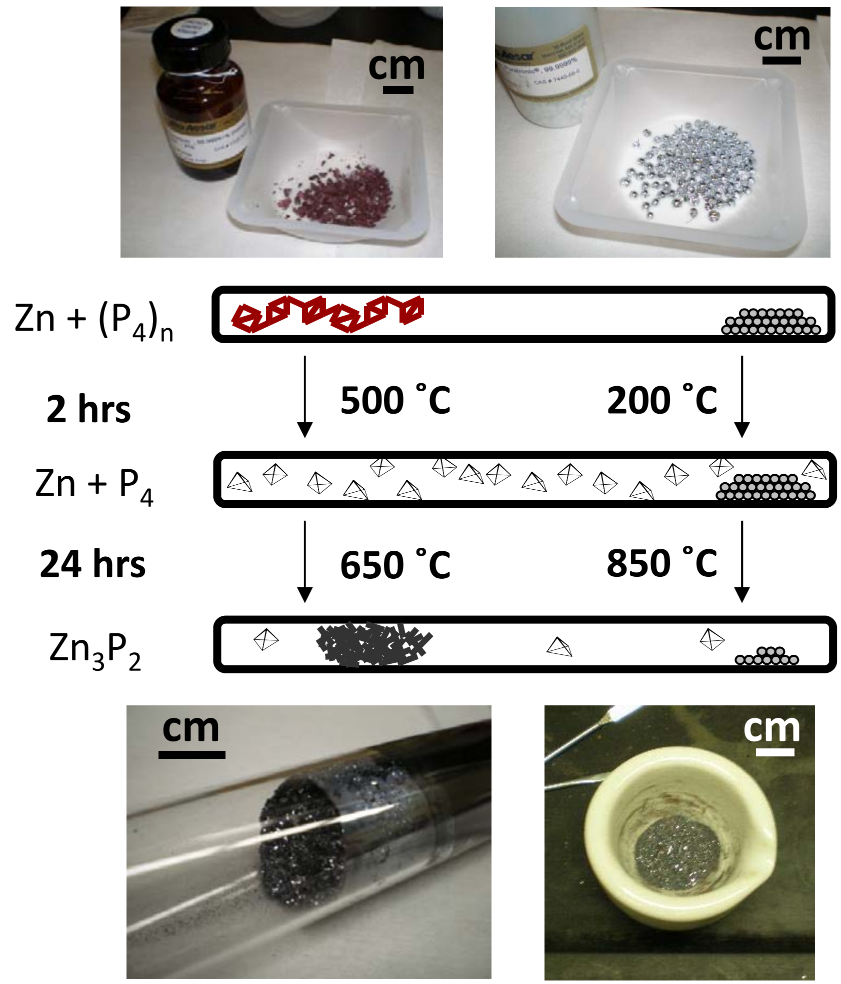

A. Catalano, *et al.* J. Crys. Growth 49, 681-686, 1980.
G. M. Kimball, A. M. Müller, N. S. Lewis, H. A. Atwater, Appl. Phys. Lett. 95, 112103, 2009.

Preparing Zn_3P_2 substrates

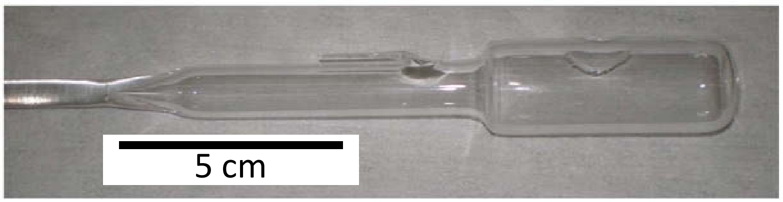

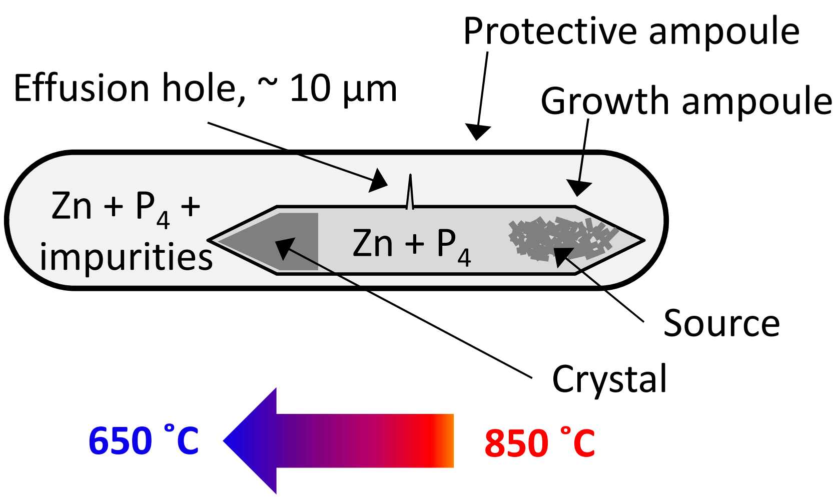

- Crystal growth by physical vapor transport (PVT) in vacuum-sealed quartz tubes
- Growth rates of 0.5 – 2.0 mm·hr^{-1}

➢ **Large-grain, quasi-single crystals**

Lapping, polishing →

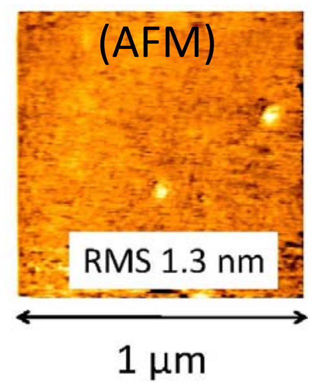

A. Catalano, *et al.* J. Crys. Growth 49, 681-686, 1980.

G. M. Kimball, A. M. Müller, N. S. Lewis, H. A. Atwater, Appl. Phys. Lett. 95, 112103, 2009.

Properties of semiconductors

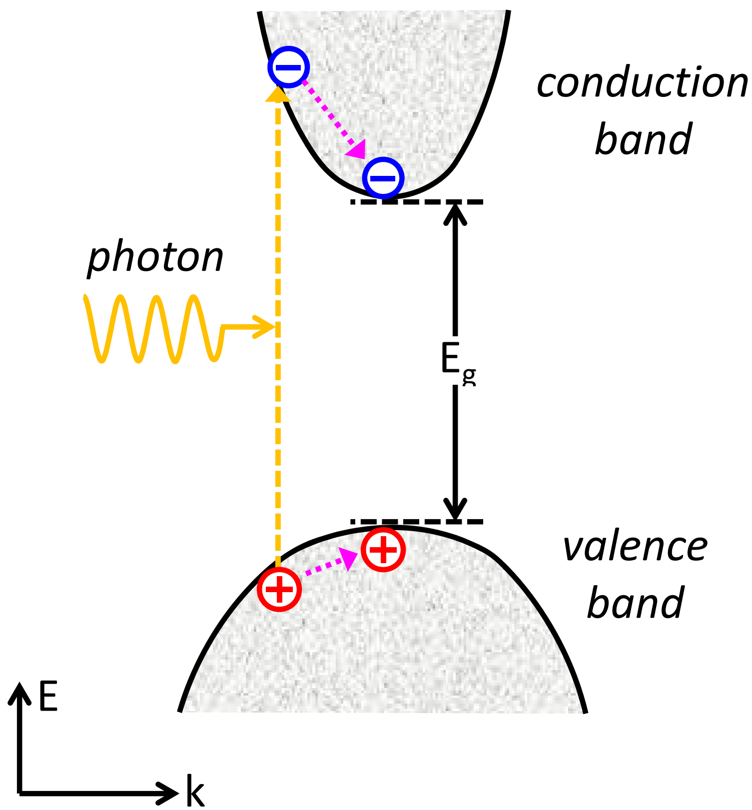

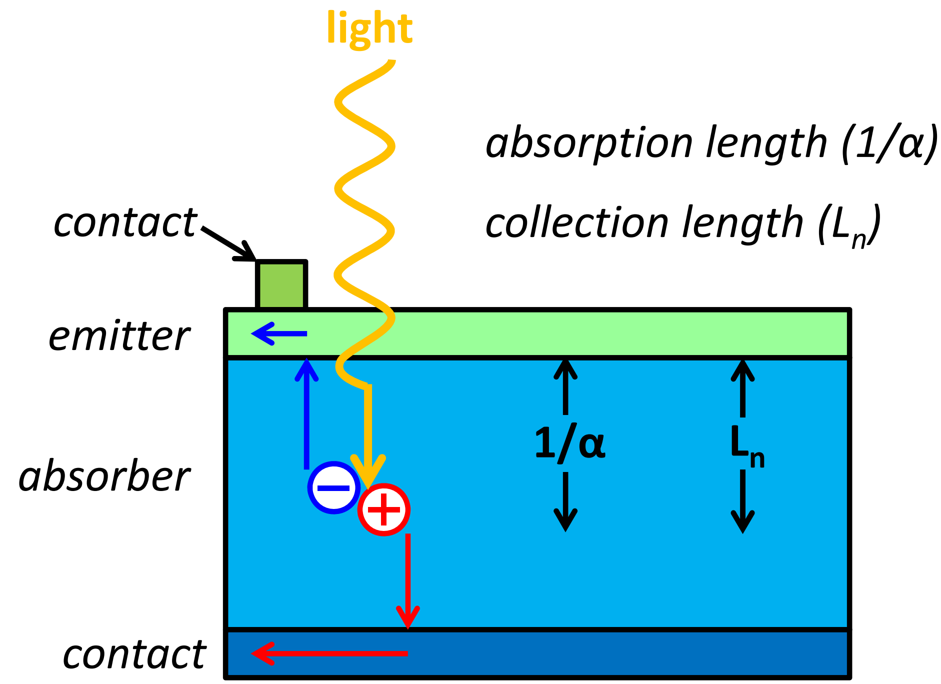

1. What is the fundamental band gap?
2. What is the absorption length? the collection length?
3. Can it be doped p-type? n-type?

Photoluminescence of semiconductors

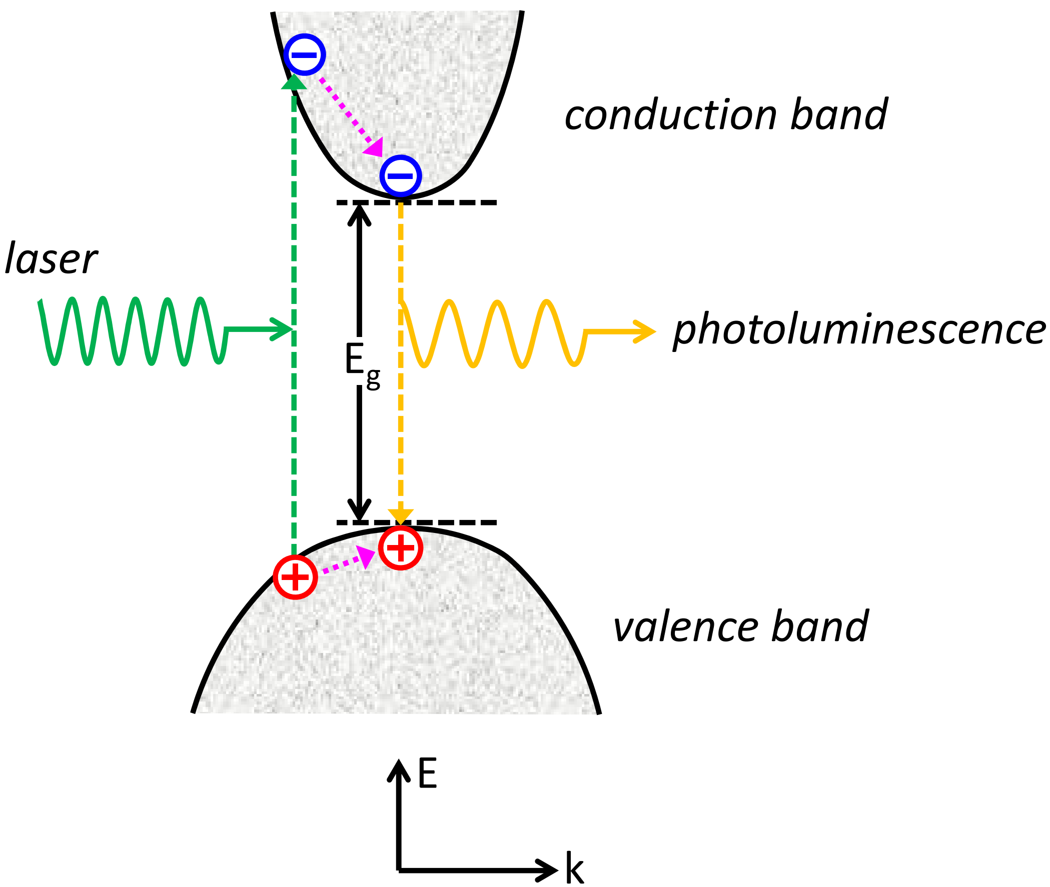

- Pump with light that is strongly absorbed
- Monitor light emission spectrum and intensity

➢ **Used to measure the band gap and to investigate carrier recombination**

G. M. Kimball, A. M. Müller, N. S. Lewis, H. A. Atwater, Appl. Phys. Lett. 95, 112103, 2009.

Temperature-dependent photoluminescence

Photoluminescence spectra

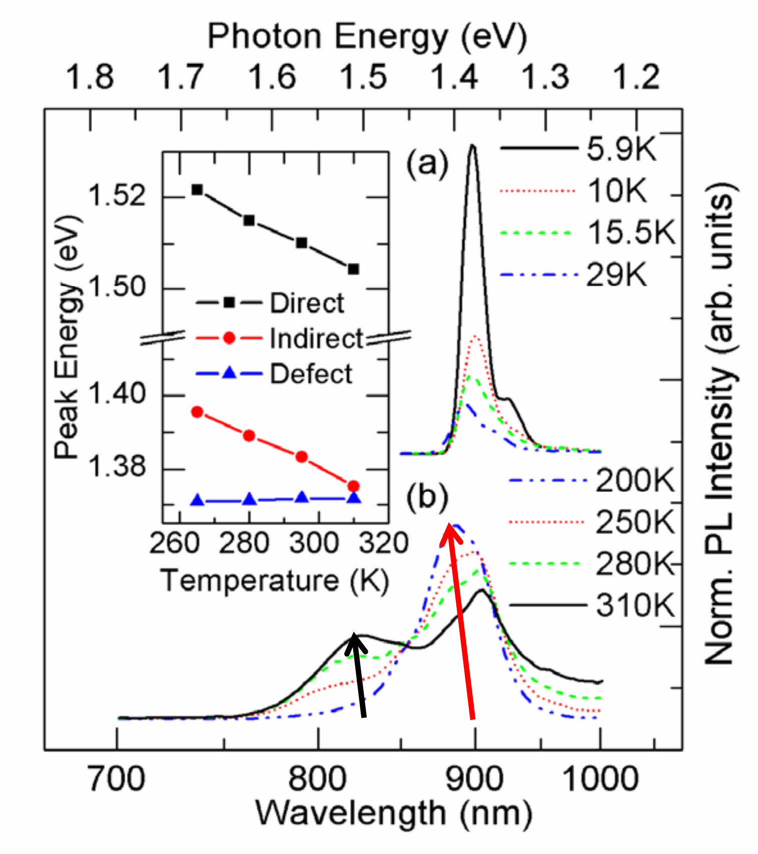

- Known direct transition at 1.50 eV
- At room temperature, the strongest emission is at 1.38 eV
- Is the luminescence due to defects or an indirect band gap?

Evidence for indirect band gap at 1.38 eV

G. M. Kimball, A. M. Müller, N. S. Lewis, H. A. Atwater, Appl. Phys. Lett. 95, 112103, 2009.

Intensity-dependent photoluminescence

- Band edge luminescence
  - Dominates at high laser intensity
  - Constant peak positions
- Defect luminescence
  - Saturates at high laser intensity
  - Peak position blue shifts

Photoluminescence spectra

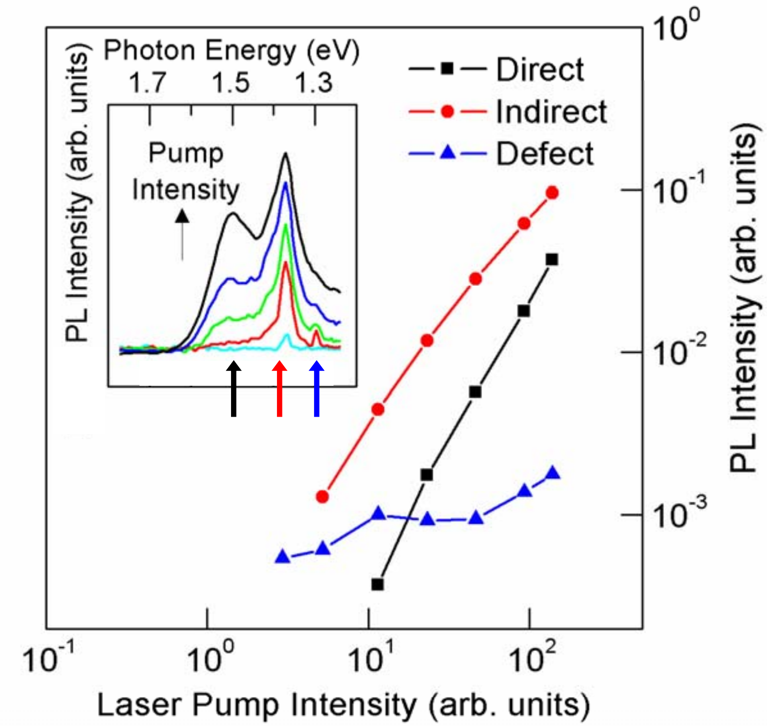

Clear evidence for indirect band gap at 1.38 eV

G. M. Kimball, A. M. Müller, N. S. Lewis, H. A. Atwater, Appl. Phys. Lett. 95, 112103, **2009**.

Band structure of Zn_3P_2

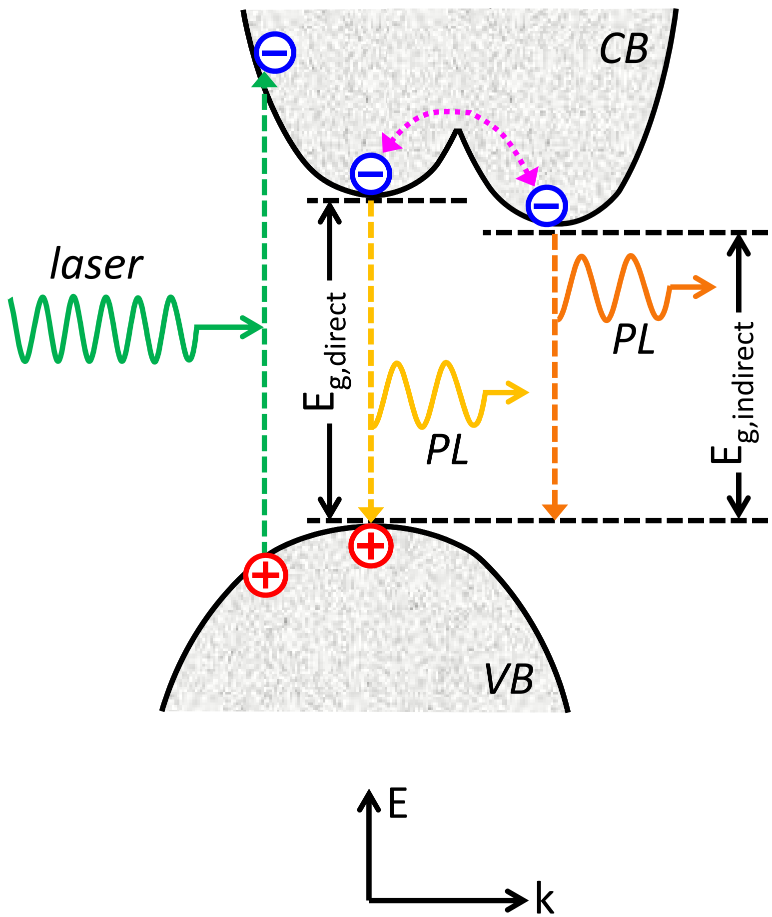

- **$E_{g,indirect}$ = 1.38 eV and $E_{g,direct}$ = 1.50 eV**
- Above 200 K there is thermal promotion of carriers from indirect to direct band gap
- Band gap values increase with cooling

G. M. Kimball, A. M. Müller, N. S. Lewis, H. A. Atwater, Appl. Phys. Lett. 95, 112103, 2009.

Analysis by spectroscopic ellipsometry

- Measured *n(ω), k(ω)* by spectroscopic ellipsometry
- Absorption coefficient:

  $\alpha\ (cm^{-1}) = 4\pi k / \lambda$

- Confirmed direct and indirect band gaps

➢ **Absorption length of 2 μm for 90% light absorption**

Real and imaginary refractive index

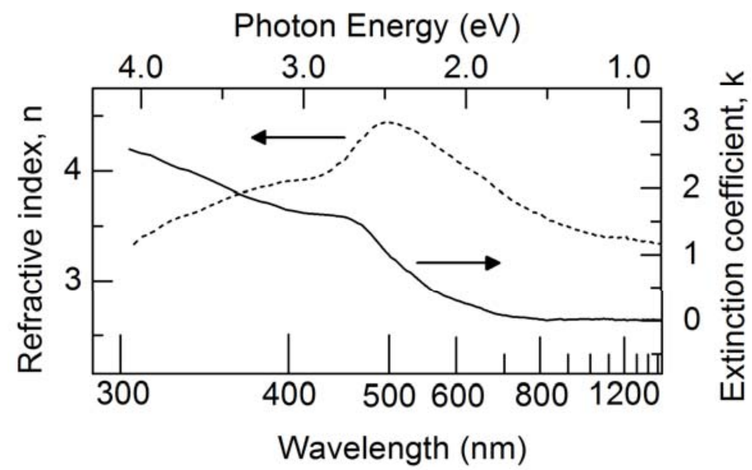

absorption spectra

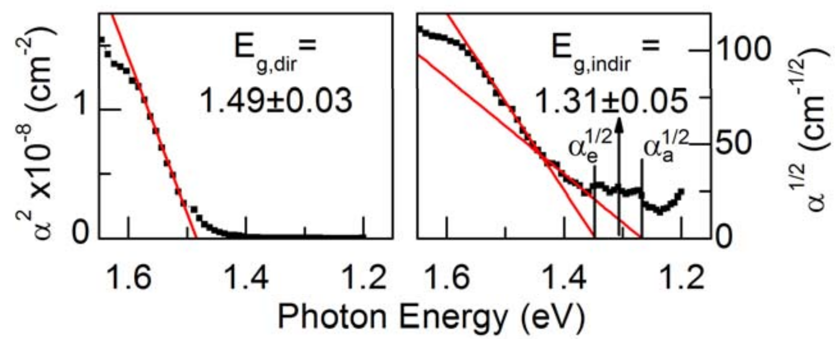

G. M. Kimball, A. M. Müller, N. S. Lewis, H. A. Atwater, Appl. Phys. Lett. 95, 112103, 2009.

Time-resolved photoluminescence

Photoluminescence decay

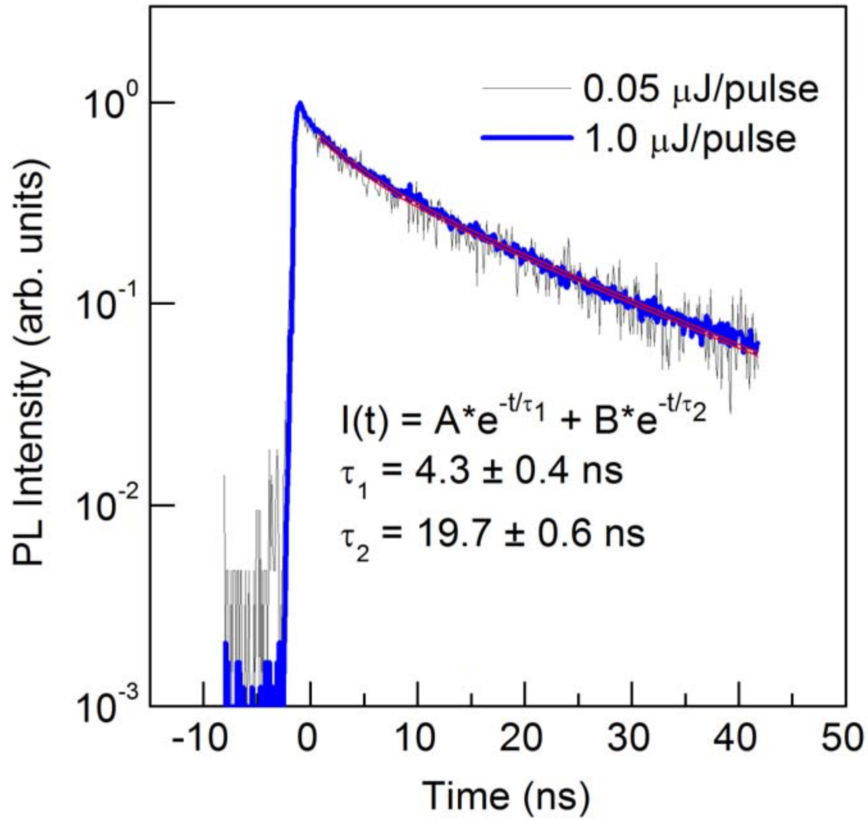

- Immediately after laser pulse, carrier recombination is surface-dominated ($\tau_{1,surface}$)
- At long times, the PL decay is limited by the bulk minority carrier lifetime ($\tau_{2,bulk}$)

Evidence for electron collection lengths ≥ 7 μm

G. M. Kimball, A. M. Müller, N. S. Lewis, H. A. Atwater, Appl. Phys. Lett. 95, 112103, 2009.

Light absorption and carrier collection

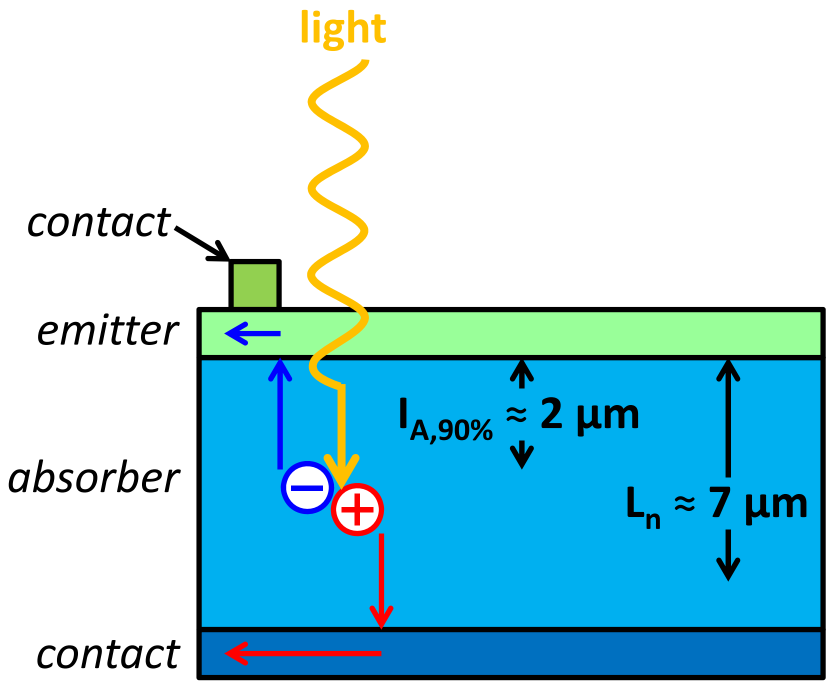

- Absorption length ≈ 2 μm for 90% light absorption
- Collection length ≈ 7 μm for efficient carrier collection

Collection lengths (7 μm) > absorption lengths (2 μm) for high quality Zn_3P_2 substrates

G. M. Kimball, A. M. Müller, N. S. Lewis, H. A. Atwater, Appl. Phys. Lett. 95, 112103, 2009.

Doping experiments and the Hall effect

- Nominally undoped substrates exhibit low p-type doping
- P and Ag act as p-type dopants

➢ **Control of p-type doping from $10^{13} – 10^{18}$ holes·cm^{-3}**

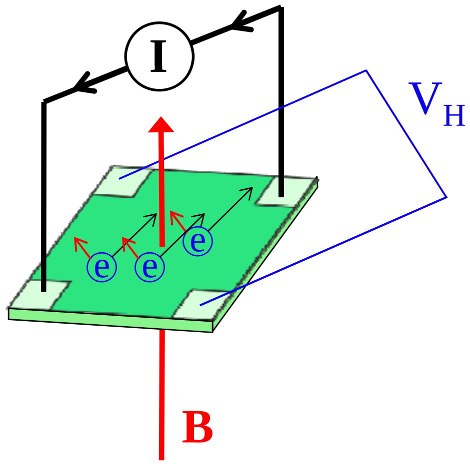

Hall effect measurements

Dopant	Anneal Ambient	p (cm^{-3})	μ_p (cm^2·V^{-1}·s^{-1})
none	none	$10^{13} – 10^{14}$	16 ± 3
none	P_4	$3.7 \pm 0.4 \times 10^{16}$	12 ± 1
Ag (1.3 nm)	P_4	$3.0 \pm 0.1 \times 10^{17}$	14 ± 1
Ag (12 nm)	P_4	$7.6 \pm 0.8 \times 10^{17}$	17 ± 2
Ag (80 nm)	P_4	$7.5 \pm 0.4 \times 10^{17}$	17 ± 1

G. M. Kimball, N. S. Lewis, H. A. Atwater. Thirty-fifth IEEE PVSC, 2010.

Cornering the market for 'Solar-Grade' Zn_3P_2

- Revealed $E_{g,indirect}$ = 1.38 eV and $E_{g,direct}$ = 1.50 eV
- Active region of ≥ 7 µm for solar energy conversion
- Control of p-type doping from $10^{13} – 10^{18}$ holes·cm^{-3}

➢ **Dominating 'Solar-Grade' Zn_3P_2 Since 2008**

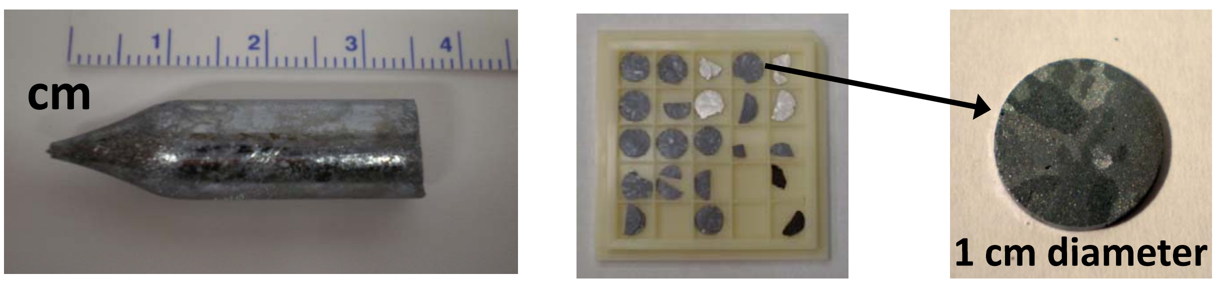

Zn_3P_2 and Cu_2O substrates for solar energy conversion

Cornering the market for 'Solar-Grade' Zn_3P_2

Why is annealing critical in Mg/Zn_3P_2 solar cells?

High performance Cu_2O/liquid junctions

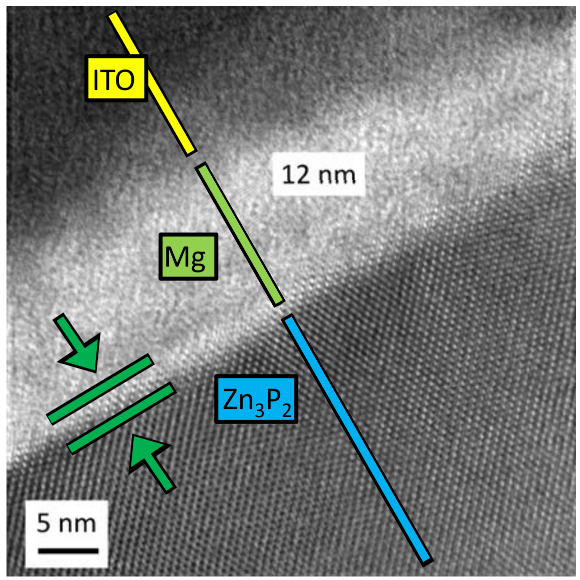

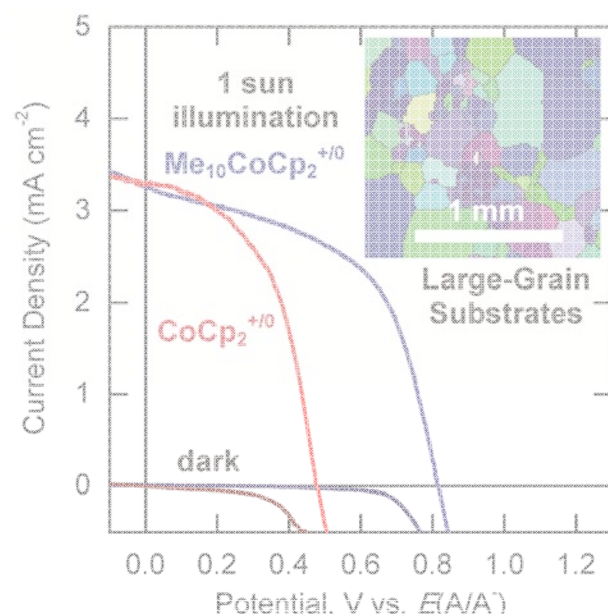

Ideal solar cell performance

Current-voltage curves

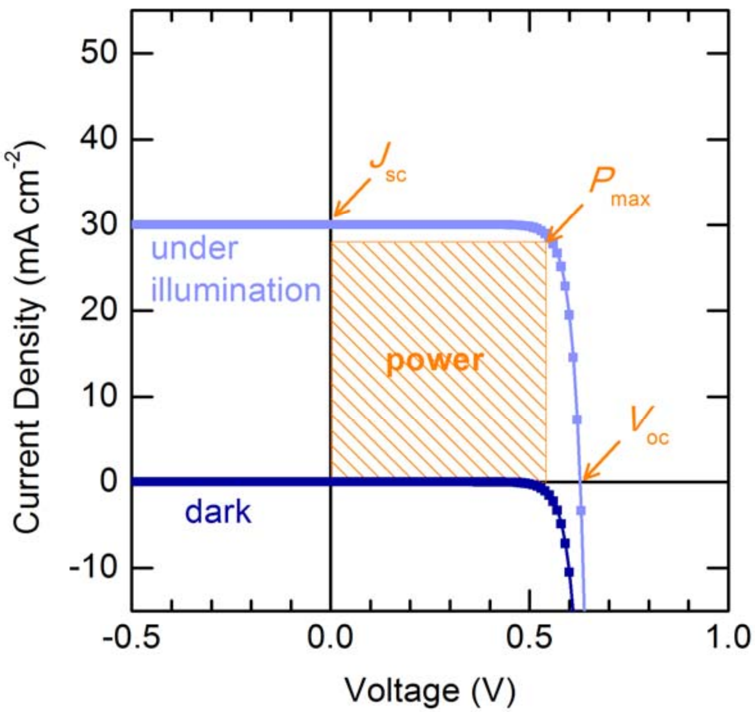

- Photons generate electron-hole pairs which are collected as current in the solar cell.
- Higher quality junctions extract more voltage for each electron-hole pair.

➢ **Improve current collection and junction quality to maximize power.**

G. M. Kimball, N. S. Lewis, H. A. Atwater, *Thirty-fifth IEEE PVSC*, 2010.

Mg/Zn_3P_2 solar cell performance

Zn_3P_2 substrates incorporated in solar cells reaching 4.5% efficiency

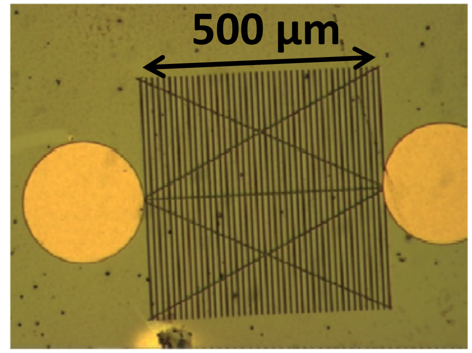

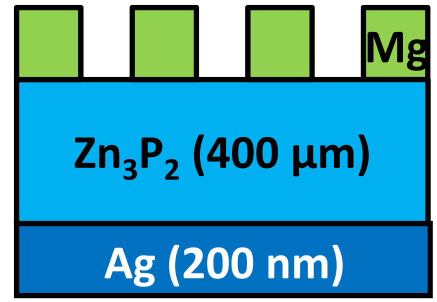

Current-voltage curves

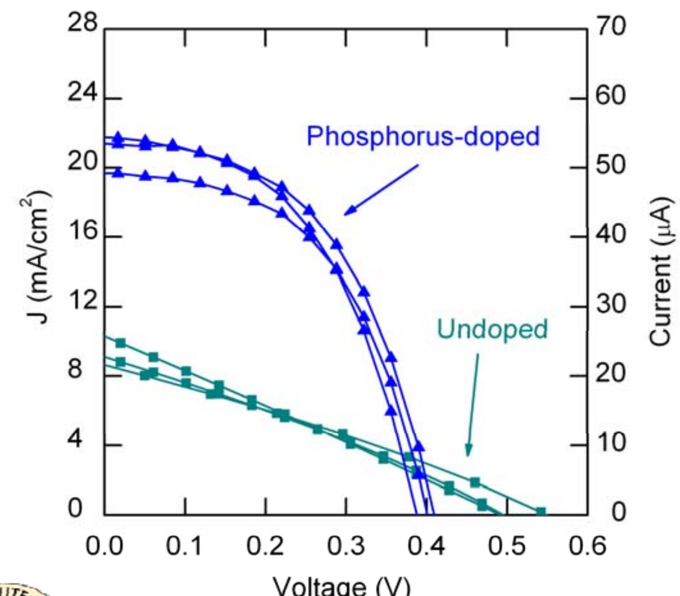

Solar cell parameters

Sample	J_{sc} (mA·cm^{-2})	V_{oc} (V)	FF	η (%)
Undoped	8.5	0.55	0.29	1.38
Undoped	10.3	0.49	0.26	1.31
Undoped	9.1	0.50	0.29	1.30
P-doped	21.8	0.39	0.50	4.20
P-doped	21.4	0.41	0.51	4.48
P-doped	19.7	0.40	0.52	4.08
Record	14.9	0.49	0.71	5.96

G. M. Kimball, N. S. Lewis, H. A. Atwater, *Thirty-fifth IEEE PVSC*, 2010.

Annealing ITO/Mg/Zn_3P_2 solar cells

- **Zn_3P_2 solar cells show large V_{oc} improvements with annealing**
- What causes the poor initial performance?
- How does annealing change the Zn_3P_2 solar cell?

V_{oc} vs annealing time

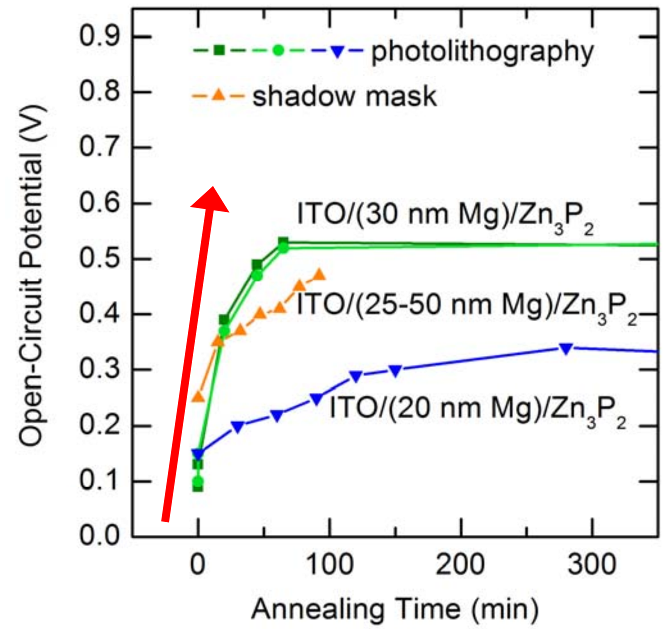

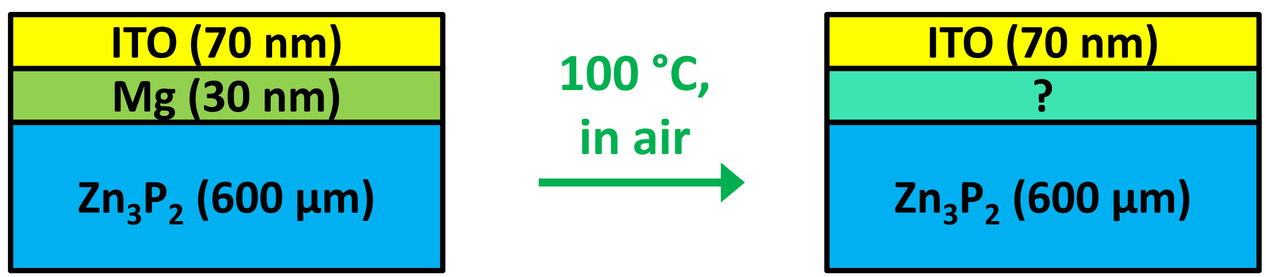

G. M. Kimball, N. S. Lewis, H. A. Atwater, *Thirty-fifth IEEE PVSC*, 2010.

Evaluating etched Zn_3P_2

X-ray photoelectron spectroscopy

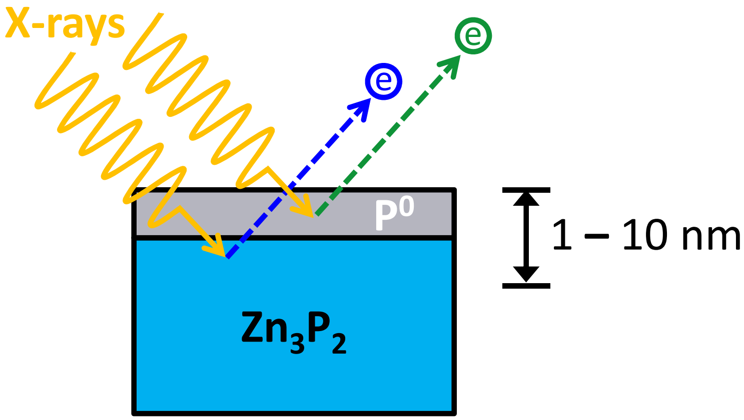

- What is the surface composition of freshly etched Zn_3P_2?
- Which elements are there and what are they bonded to?

➢ **X-ray photoelectron spectroscopy (XPS) probes the first 1 – 10 nm of surface atoms**

G. M. Kimball, N. S. Lewis, H. A. Atwater, *Thirty-third IEEE PVSC*, 2008.
G. M. Kimball, (in preparation), 2011.

Evaluating etched Zn_3P_2

X-ray photoelectron spectroscopy

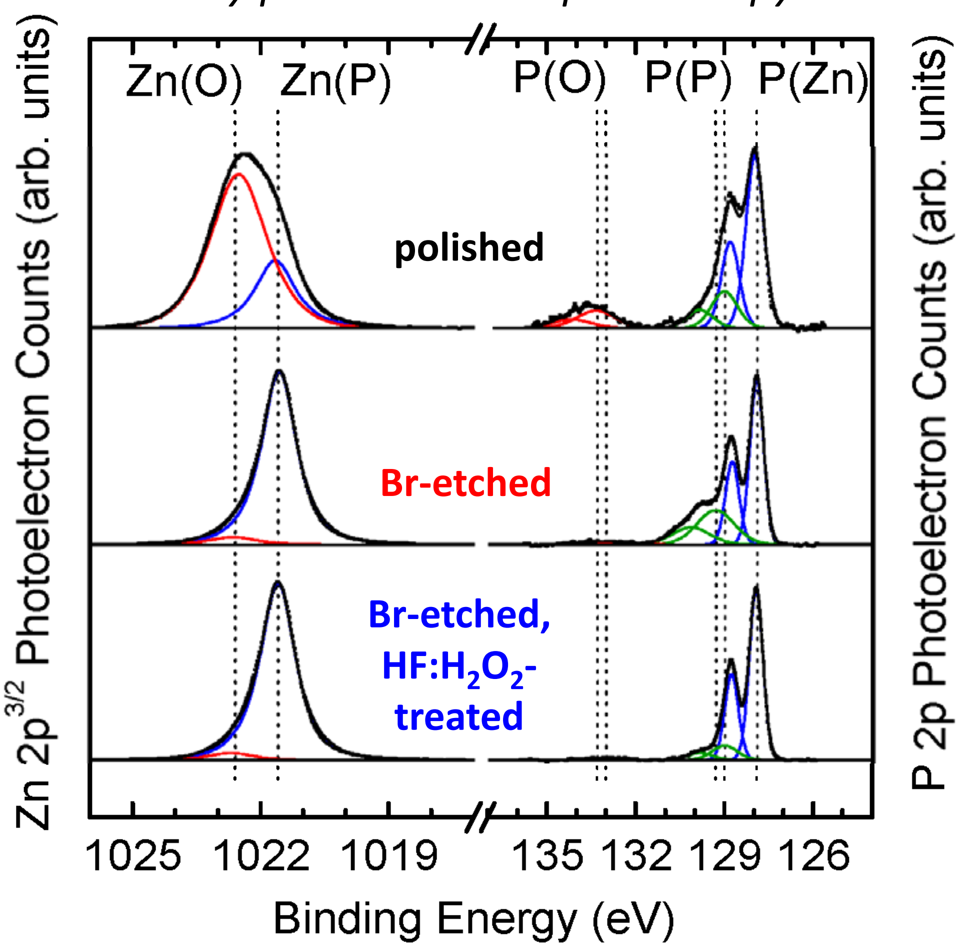

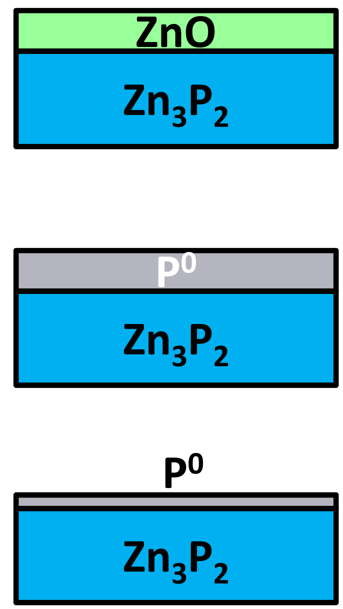

Polished substrates exhibit zinc-rich oxidation

Br_2:MeOH etching leaves 4 – 5 monolayers P^0

$HF:H_2O_2$ (aq) selectively removes the P^0 residue

G. M. Kimball, N. S. Lewis, H. A. Atwater, *Thirty-third IEEE PVSC*, 2008.
G. M. Kimball, (in preparation), 2011.

Evaluating etched Zn_3P_2

- Br_2:MeOH etching enables room temperature PL measurements
- $HF:H_2O_2$ (aq) treatment enhances PL intensity
- **Removal of surface P^0 correlates with fewer surface defects**

Photoluminescence decays and spectra

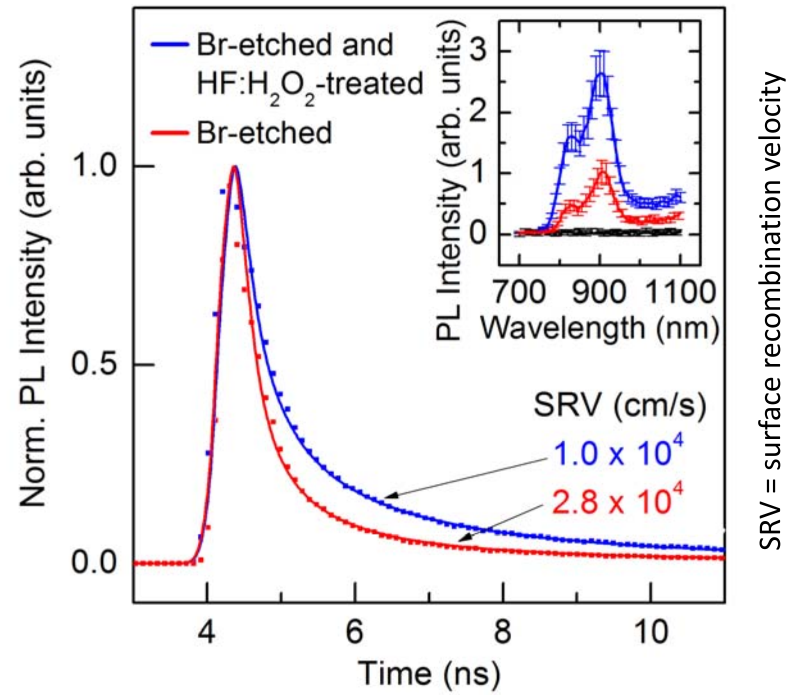

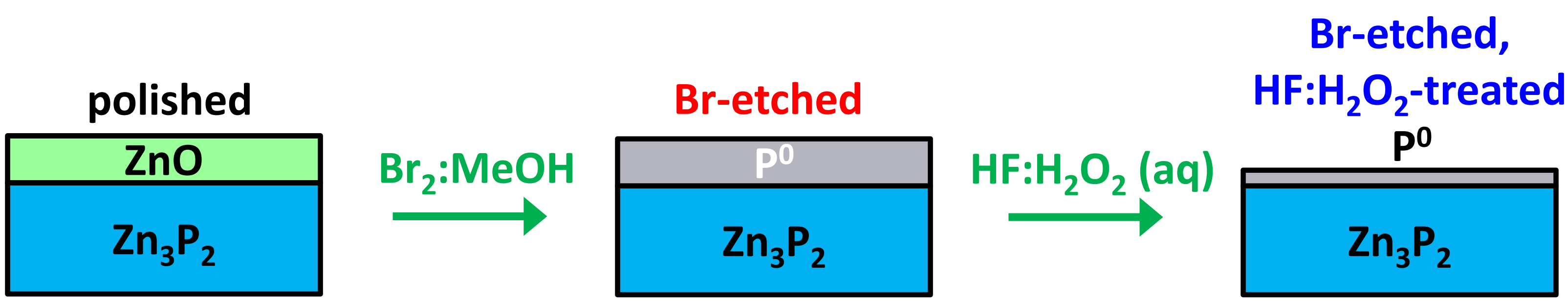

Why is annealing critical?

As-fabricated,
V_{oc} less than 100 mV

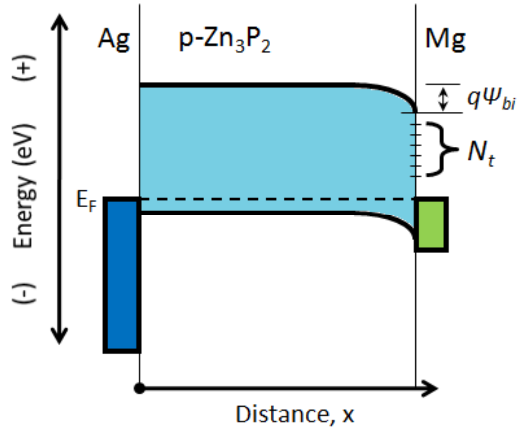

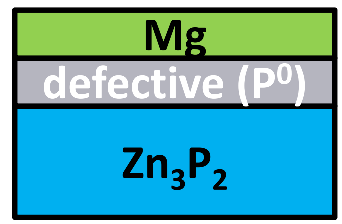

?

Anneal, 100 °C

?

?

(A) n-Zn_3P_2/Zn_3P_2
p-n homojunction

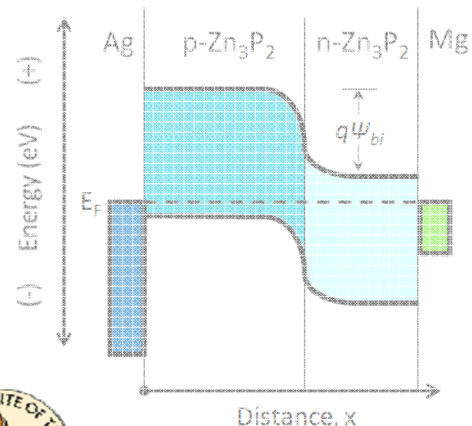

(B) Mg_xZn_yP/Zn_3P_2
p-n heterojunction

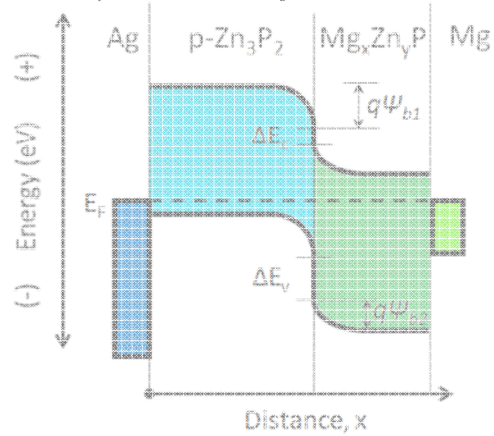

(C) Passivated
Mg/Zn_3P_2 Schottky

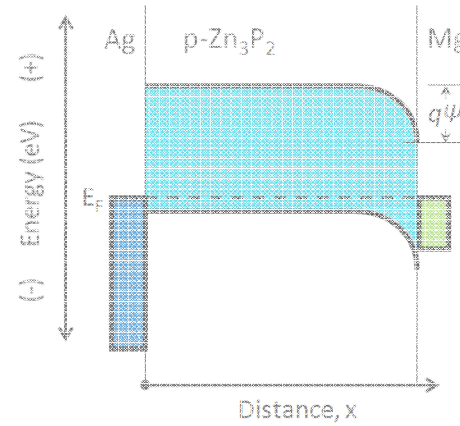

Why is annealing critical?

As-fabricated,
V_{oc} less than 100 mV

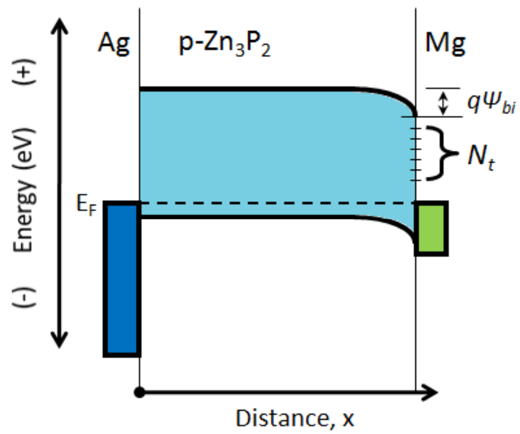

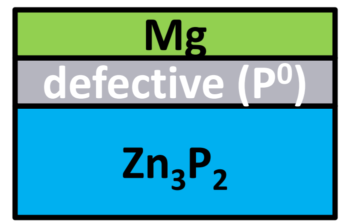

?

Anneal, 100 °C

?

?

(A) n-Zn_3P_2/Zn_3P_2
p-n homojunction

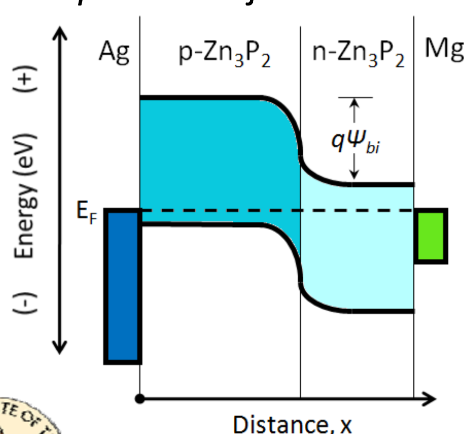

(B) Mg_xZn_yP/Zn_3P_2
p-n heterojunction

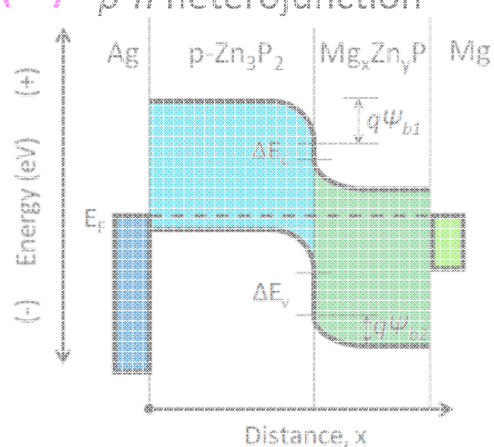

(C) Passivated
Mg/Zn_3P_2 Schottky

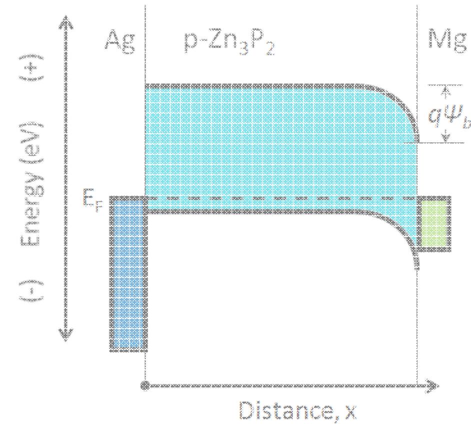

Why is annealing critical?

As-fabricated,
V_{oc} less than 100 mV

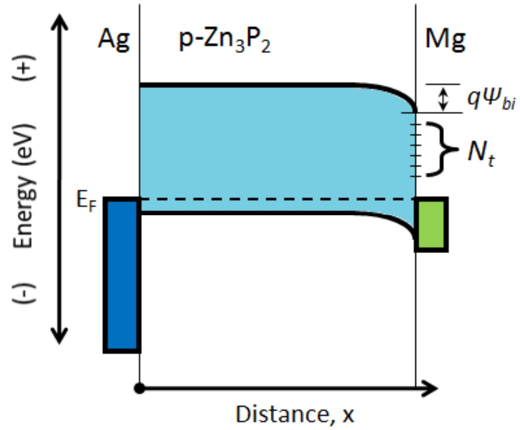

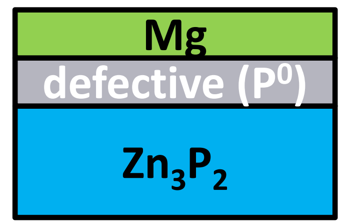

Anneal, 100 °C

(A) n-Zn_3P_2/Zn_3P_2
p-n homojunction

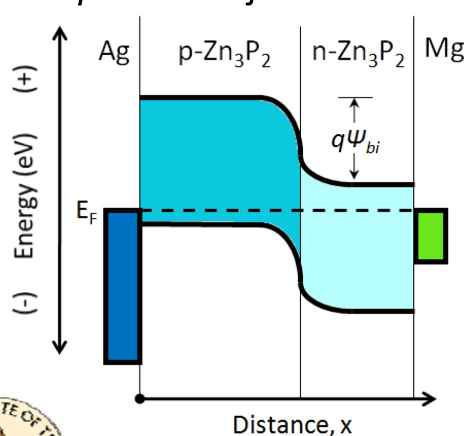

(B) Mg_xZn_yP/Zn_3P_2
p-n heterojunction

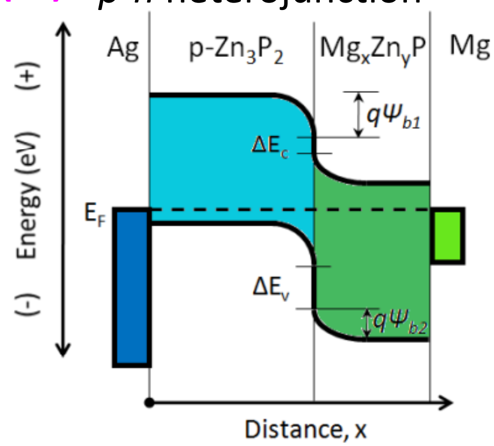

(C) Passivated
Mg/Zn_3P_2 Schottky

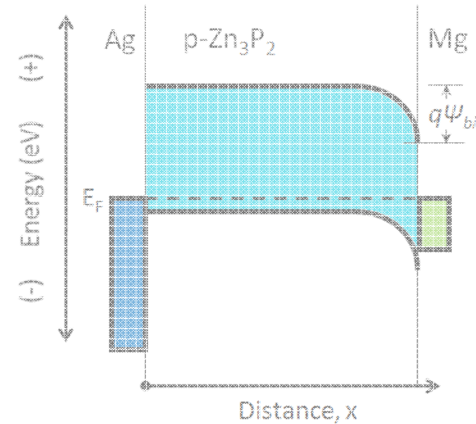

Why is annealing critical?

As-fabricated,
V_{oc} less than 100 mV

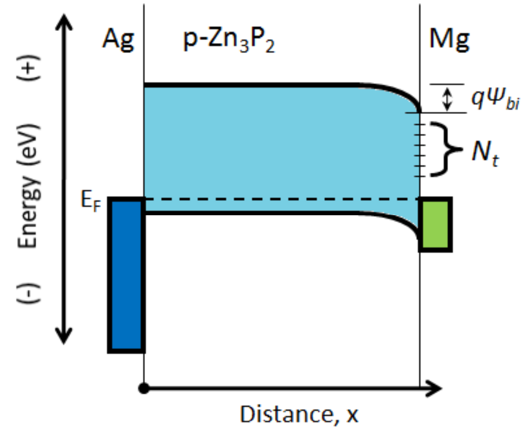

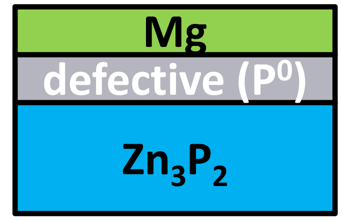

? **Anneal, 100 °C** ? ?

(A) n-Zn_3P_2/Zn_3P_2
p-n homojunction

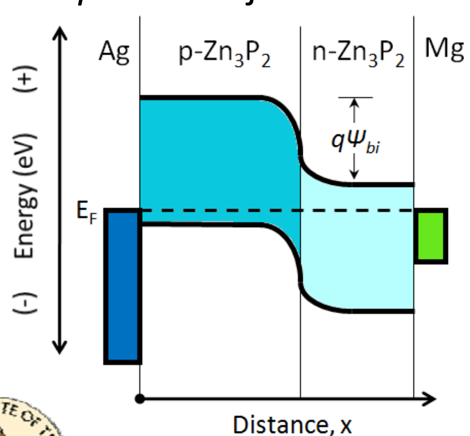

(B) Mg_xZn_yP/Zn_3P_2
p-n heterojunction

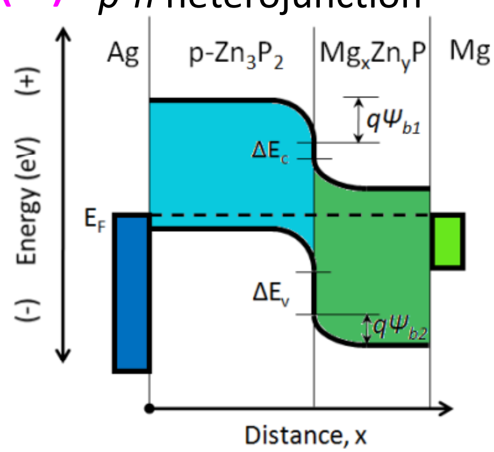

(C) Passivated
Mg/Zn_3P_2 Schottky

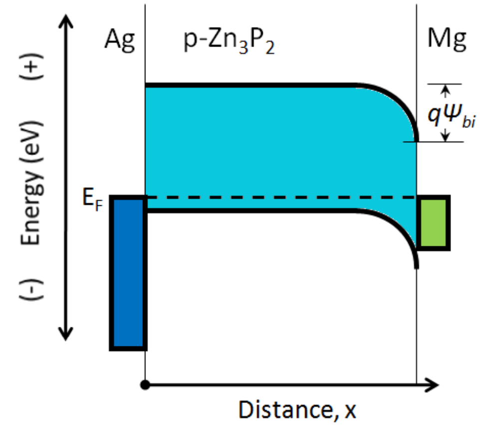

(A) Evaluating Mg-doped Zn_3P_2

- Mg diffuses readily into Zn_3P_2
- Substrates with Mg impurities were resistive with low p-type conductivity

➢ ***p-n* homojunction formation is unlikely**

Secondary Ion Mass Spectrometry

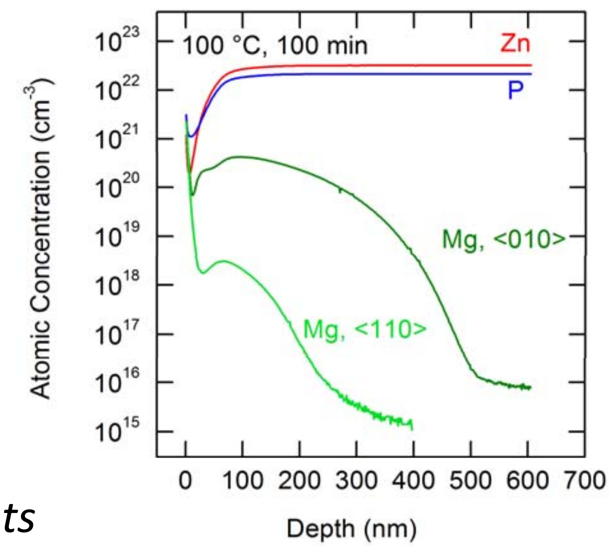

p-n homojunction?

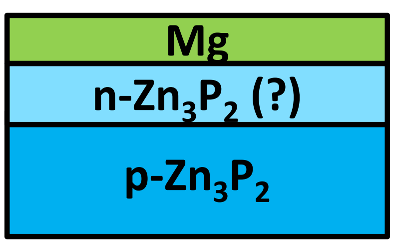

Hall effect measurements

Dopant	Anneal Ambient	p (cm^{-3})	μ_p ($cm^2 \cdot V^{-1} \cdot s^{-1}$)
none	none	$10^{13} – 10^{14}$	16 ± 3
none	P_4	$3.7 \pm 0.4 \times 10^{16}$	12 ± 1
Mg (80 nm)	P_4	$3.8 \pm 0.8 \times 10^{13}$	19 ± 3
Mg (80 nm)	P_4 + Mg	$5.4 \pm 0.8 \times 10^{13}$	41 ± 18
Mg (80 nm)	Vacuum	$6.0 \pm 3.2 \times 10^{12}$	48 ± 25
Mg (80 nm)	Mg	$1.5 \pm 0.4 \times 10^{14}$	9 ± 2

G. M. Kimball, N. S. Lewis, H. A. Atwater, *Thirty-fifth IEEE PVSC*, 2010.

(B)

Evaluating Mg-Zn-P Heterojunctions

TEM analysis shows abrupt (< 5 nm) interface in ITO/Mg/Zn_3P_2 solar cells

p-n heterojunction?

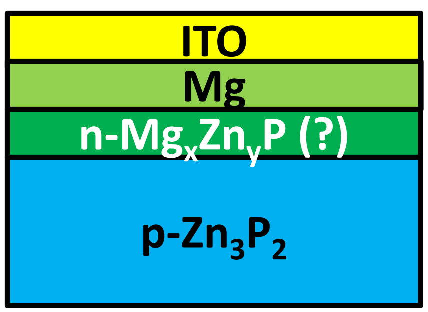

Transmission electron microscopy cross-section

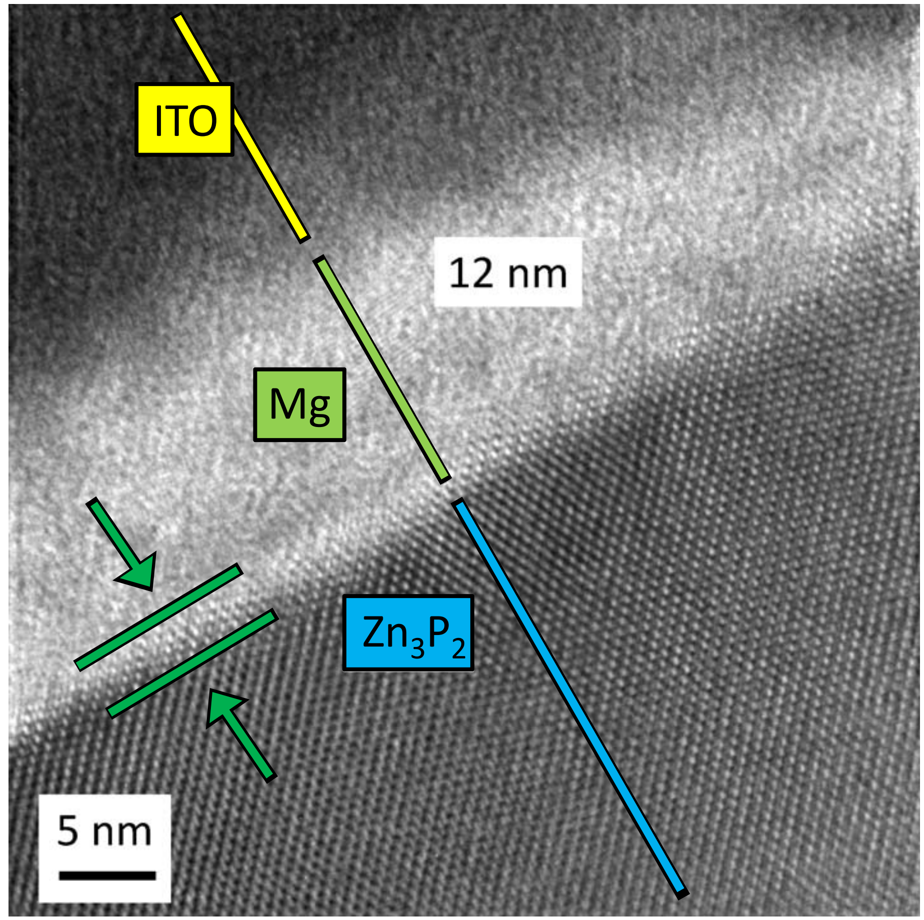

Image: Steve Rozeveld

Annealed at 100 °C in air for 100 min

G. M. Kimball, (in preparation), 2011.

(C)

Evaluating Mg passivation

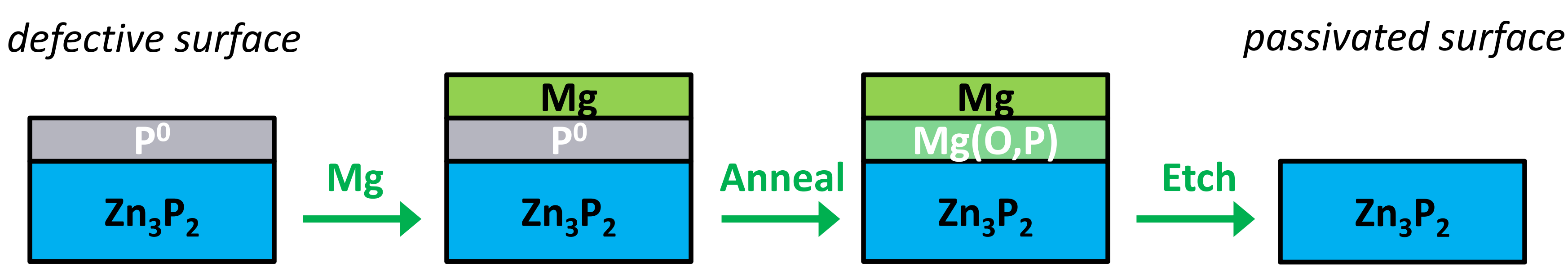

- Freshly etched Zn_3P_2 has a defective surface
- **Mg/Zn_3P_2 undergoes a solid-state passivation reaction that improves V_{oc}**
- Passivated Zn_3P_2 can then be incorporated into solar cell

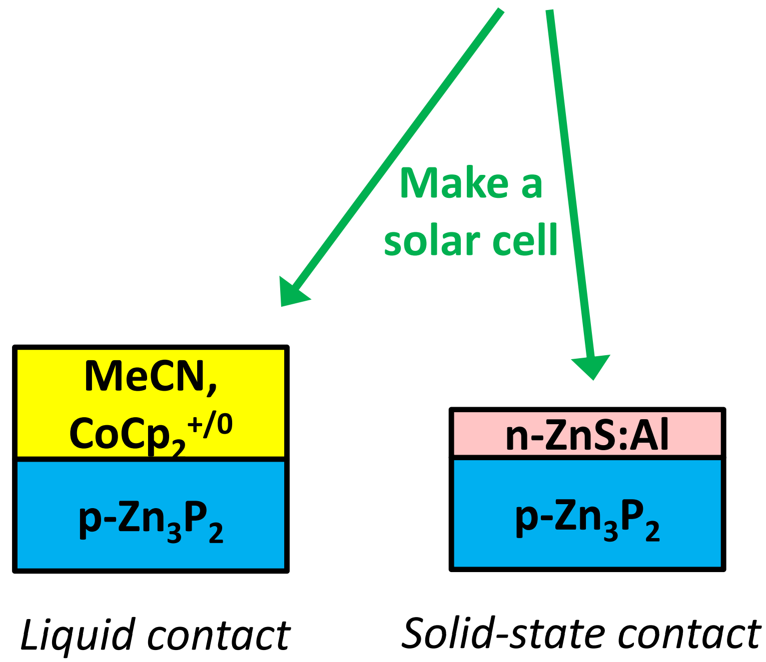

Mg (200 nm) deposited on Br-etched Zn_3P_2, annealed at 100 °C for 90 min, and removed in 10 mM EDTA/10% H_2O_2 (aq, pH 10).

G. M. Kimball, (in preparation), 2011.

(C)

Surface analysis of Mg passivation

(a) Etched with Br_2:MeOH

(b) Mg treated, etched with EDTA (aq), 15 sec

(c) Mg treated, etched with EDTA:H_2O_2 (aq), 60 sec

Mg treatment appears to remove (P^0) and surface defects

X-ray photoelectron spectroscopy

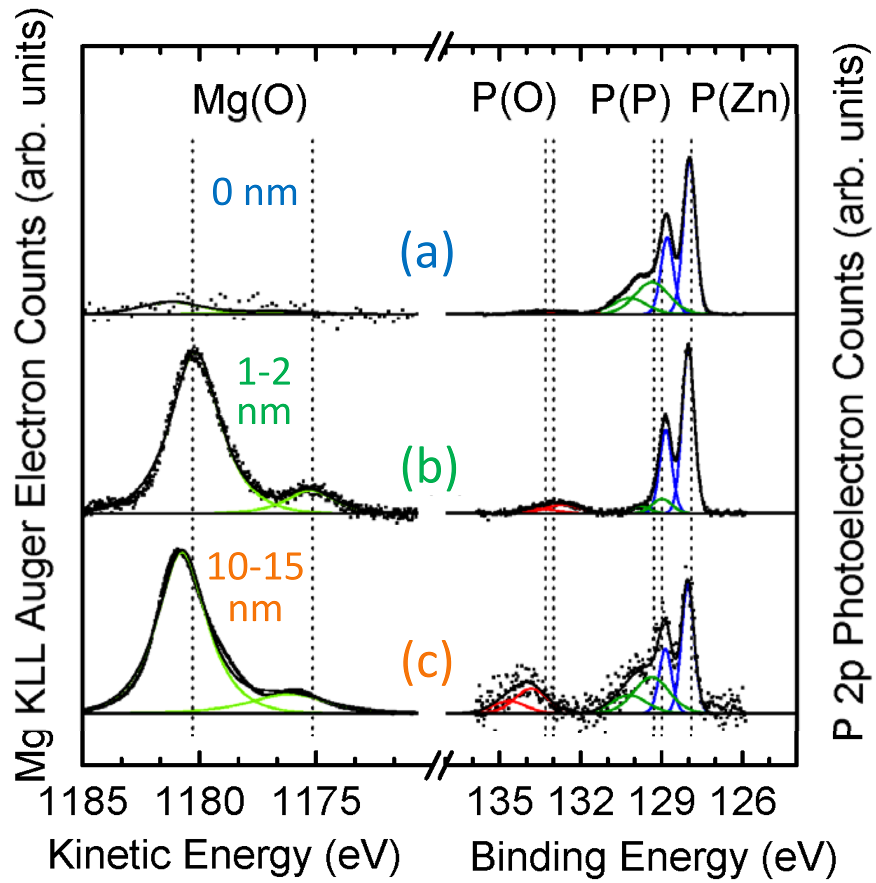

Mg treatment:

1. Br-etched Zn_3P_2 metallized with 200 nm Mg
2. Substrates annealed at 100 °C for 90 min
3. Mg removed in 10 mM EDTA/10% H_2O_2 (aq, pH 10).

G. M. Kimball, (in preparation), 2011.

(C) Effect of Mg treatment

V_{oc} for pulsed light

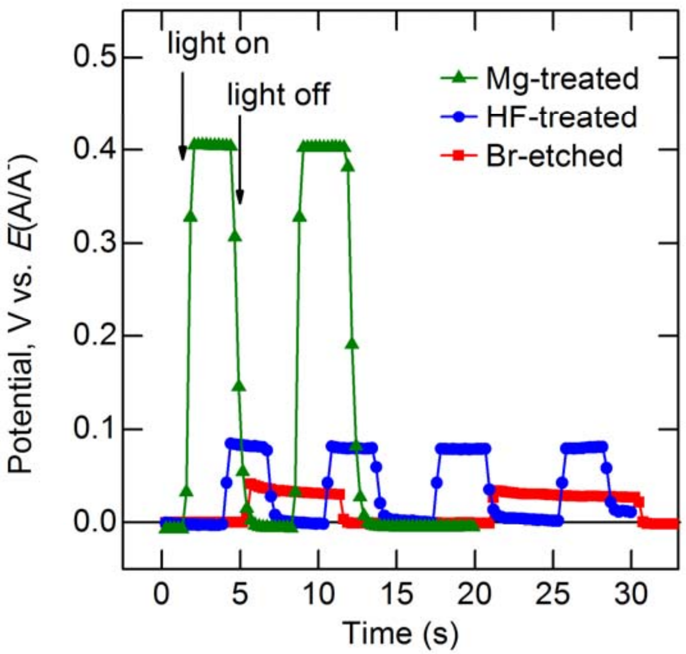

Current-voltage curves

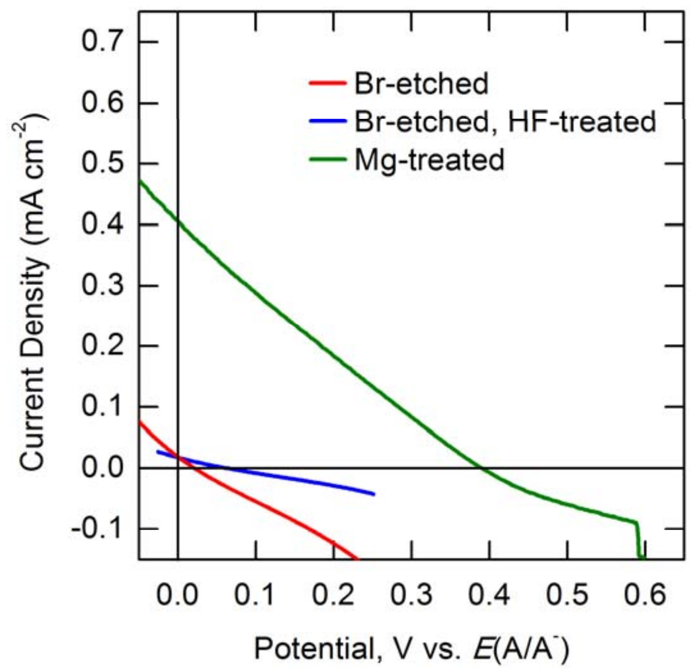

- Freshly etched Zn_3P_2 yields V_{oc} values < 100 mV
- **Mg-treatment yields V_{oc} values reaching 400 mV**
- Residual MgO introduces significant series resistance

G. M. Kimball, (in preparation), 2011.

The Future of Zn_3P_2 passivation

- Nonaqueous Mg etching chemistry to reduce the formation of resistive MgO
- Reactive metals other than Mg to yield more complete passivation with fewer side effects

➢ **Mg passivation opens up new approaches to high performance Zn_3P_2 solar cells!**

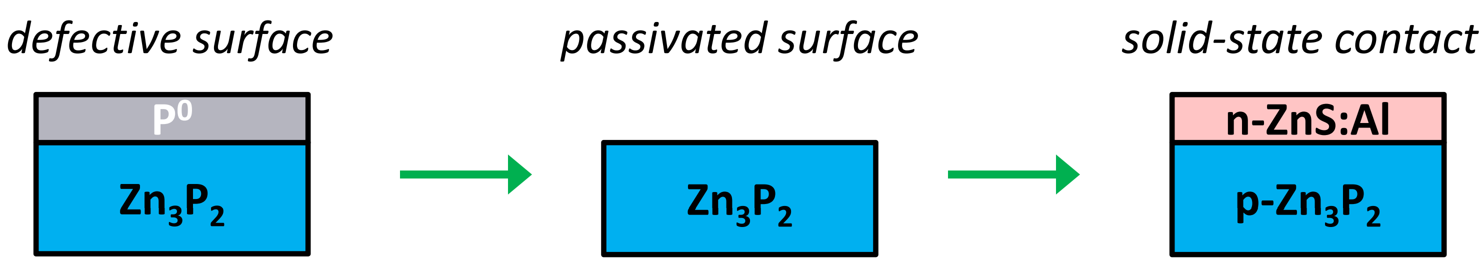

Zn_3P_2 and Cu_2O substrates for solar energy conversion

Cornering the market for 'Solar-Grade' Zn_3P_2

Why is annealing critical in Mg/Zn_3P_2 solar cells?

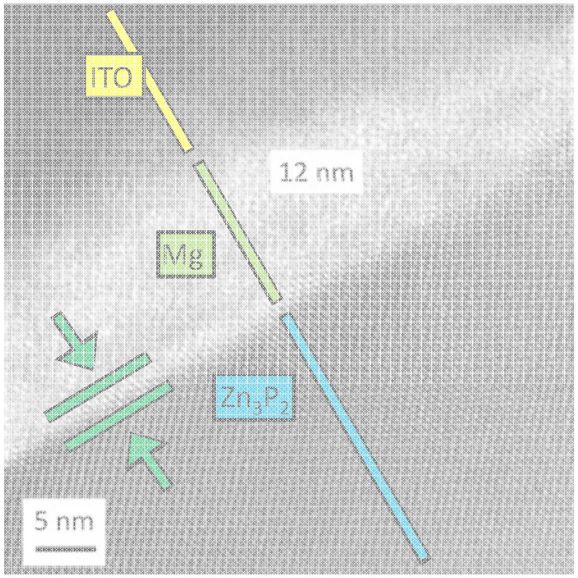

High performance Cu_2O/liquid junctions

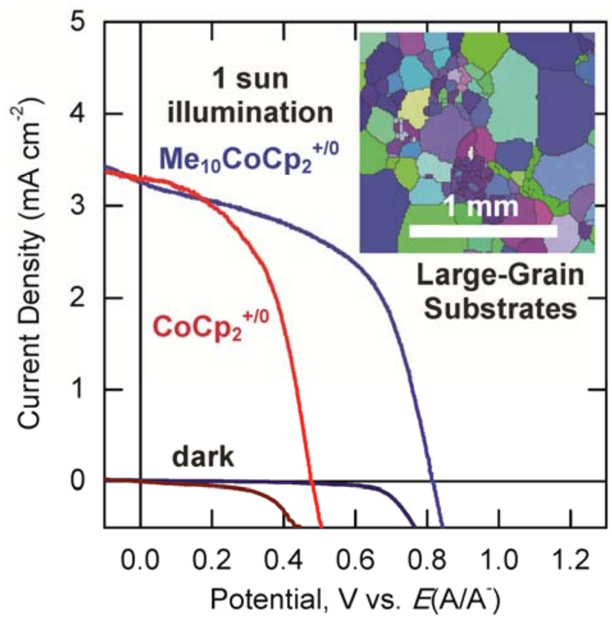

Cu_2O: Wide Band Gap Material

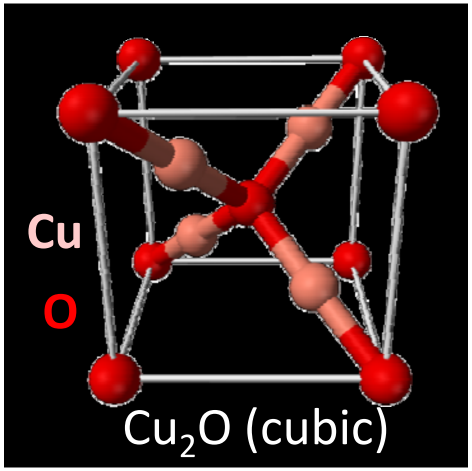

Progress from the 1980s

- Direct band gap at 2.0 eV
- Cu/Cu_2O diodes of 1.8% efficiency
- Oxidized from Cu metal
- Promising for two-junction solar cell

Wyckoff, R. W. G.: Crystal Structures, Vol. 1, 2nd Edition, J. Wiley, New York, 1965.
L. C. Olsen, W. Miller, Solar Cells, 7, 247 – 279, 1982.

Are stable, high barrier contacts possible?

Barrier height vs expected

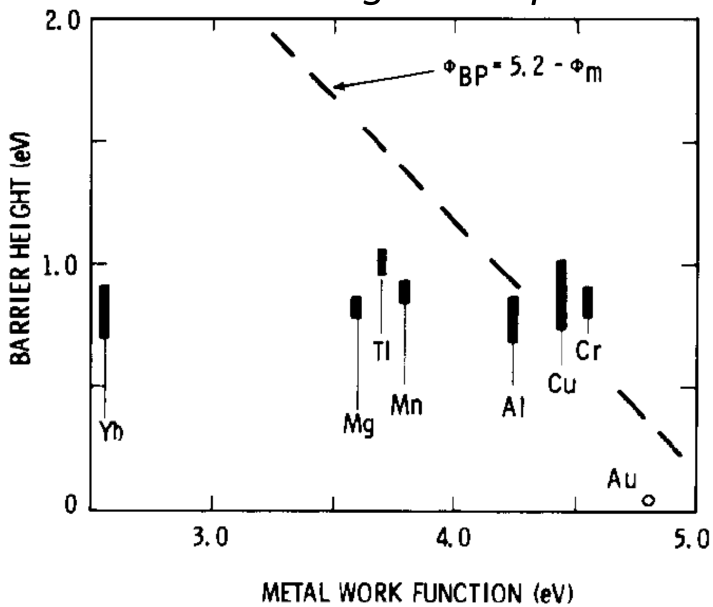

- Cu precipitation limits the V_{oc} to 300 – 400 mV in Cu_2O diodes
- Occurs spontaneously at reducing interfaces

➢ **Preventing interfacial Cu would allow higher performance**

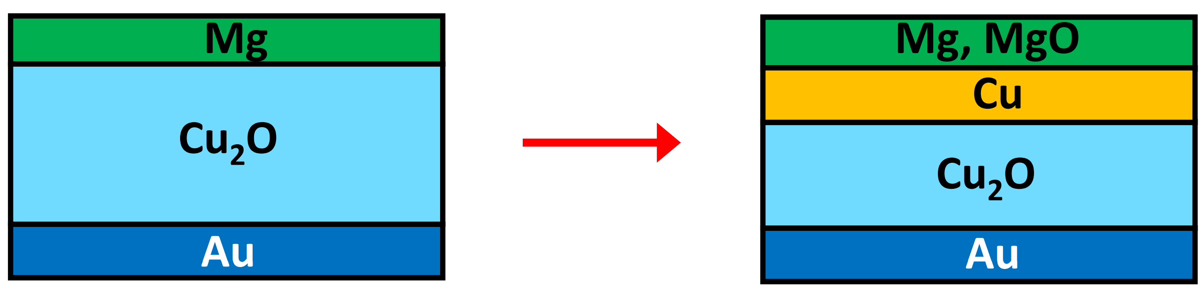

L. C. Olsen, R. C. Bohara, M. W. Urie, Appl. Phys. Lett. 34, 1, 1979.
L. C. Olsen, W. Miller, Solar Cells, 7, 247 – 279, 1982.

Cu_2O from the elements

Cu-O phase diagram

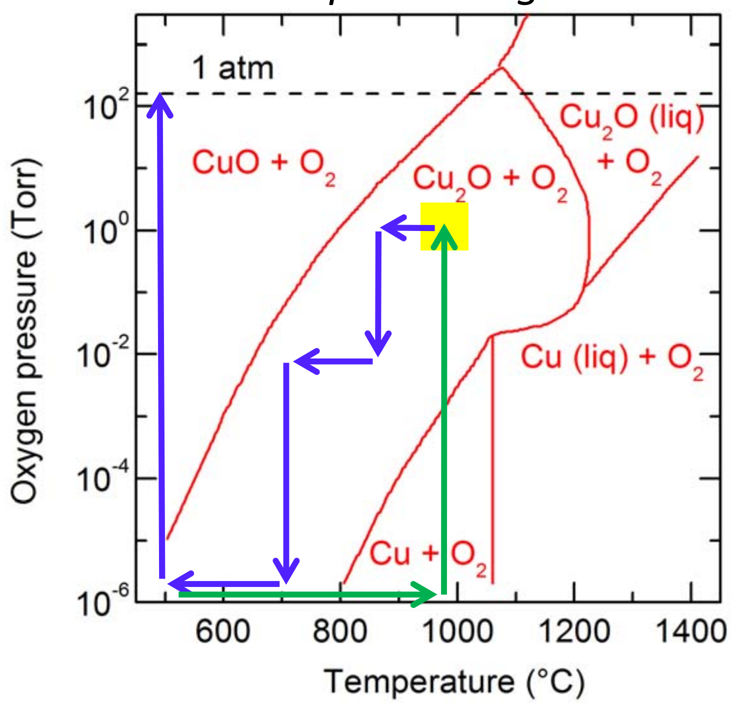

980 °C, 6 Torr O_2 for 2 hrs

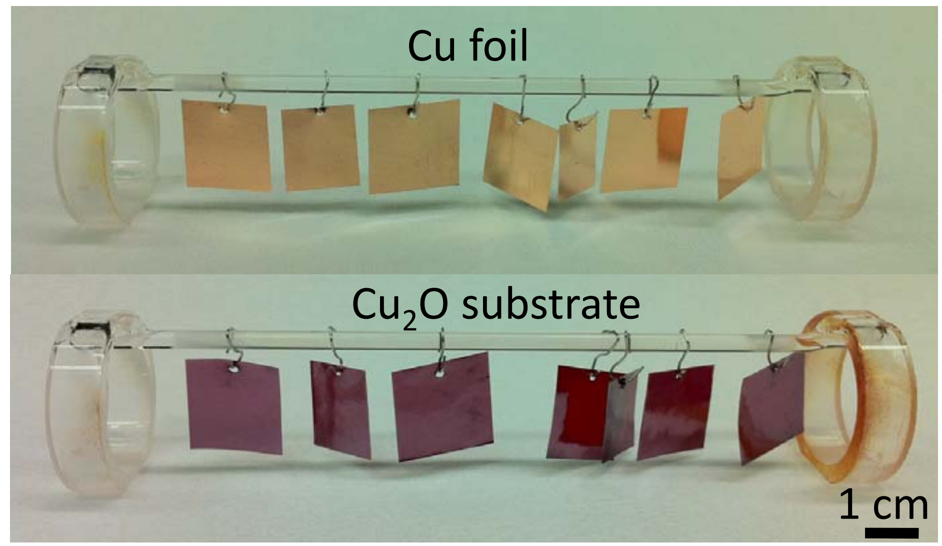

Cu_2O substrates from the thermal oxidation of 99.9999% Cu foils

C. Xiang, **G. M. Kimball**, R. Grimm, N. S. Lewis. En. & Env. Sci. DOI: 10.1039/c0ee00554a, 2011.

High purity Cu_2O substrates

SEM image

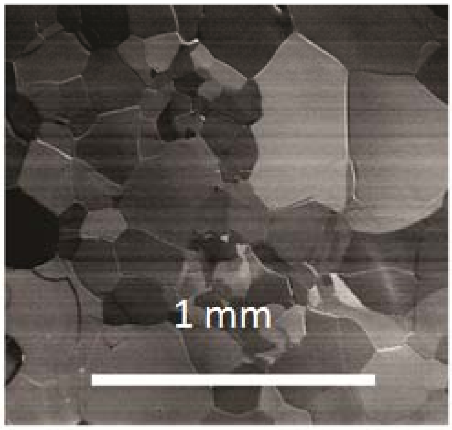

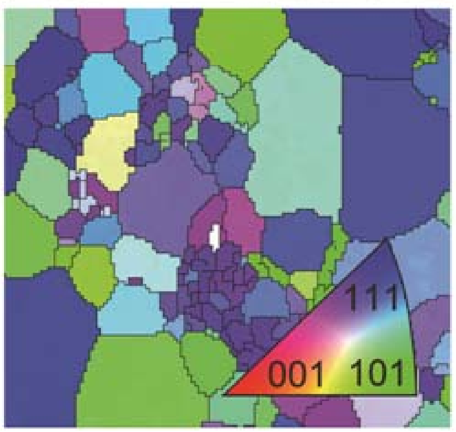

Crystal orientation

X-ray diffraction

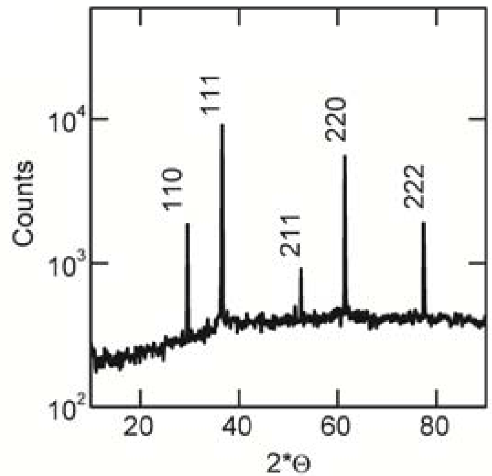

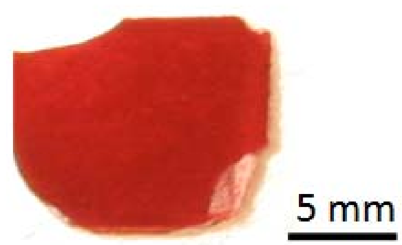

Electronic properties:

N_A = 3.7 x 10^{13} cm^{-3}

μ_p = 65 $cm^2 \cdot V^{-1} \cdot s^{-1}$

High quality, large grain Cu_2O substrates

C. Xiang, **G. M. Kimball**, R. Grimm, N. S. Lewis. En. & Env. Sci. DOI: 10.1039/c0ee00554a, 2011.

Photoelectrochemistry of semiconductors

Schematic of PEC cell

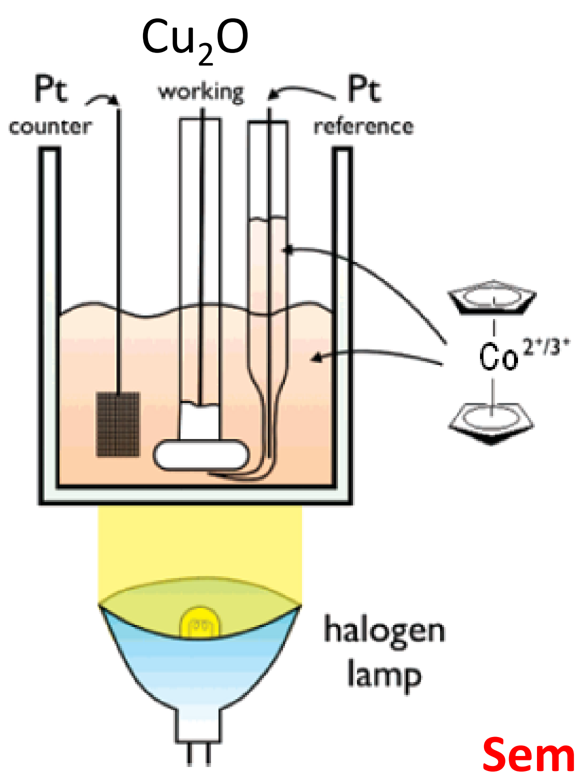

Band diagram of PEC cell

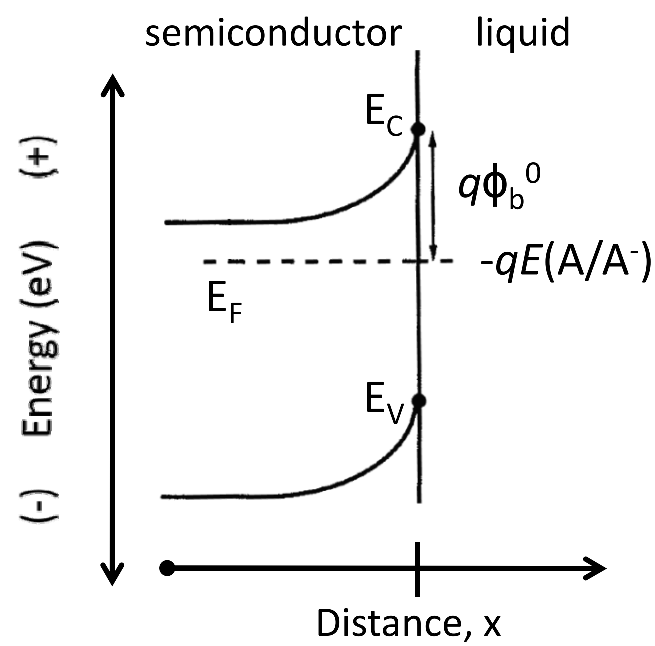

Semiconductor/liquid junctions allow noninvasive characterization of semiconductor absorbers

Image: J. R. Maiolo

Performance of Cu_2O liquid junctions

Current-voltage curves

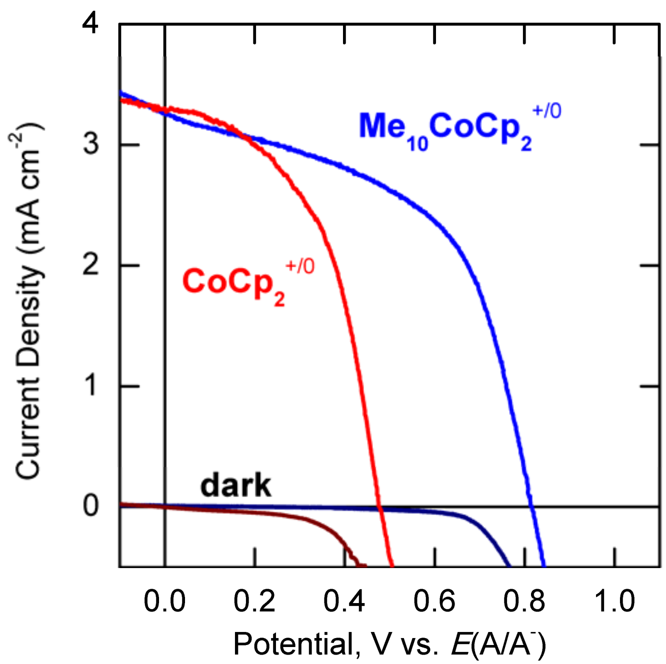

Quantum yield spectra

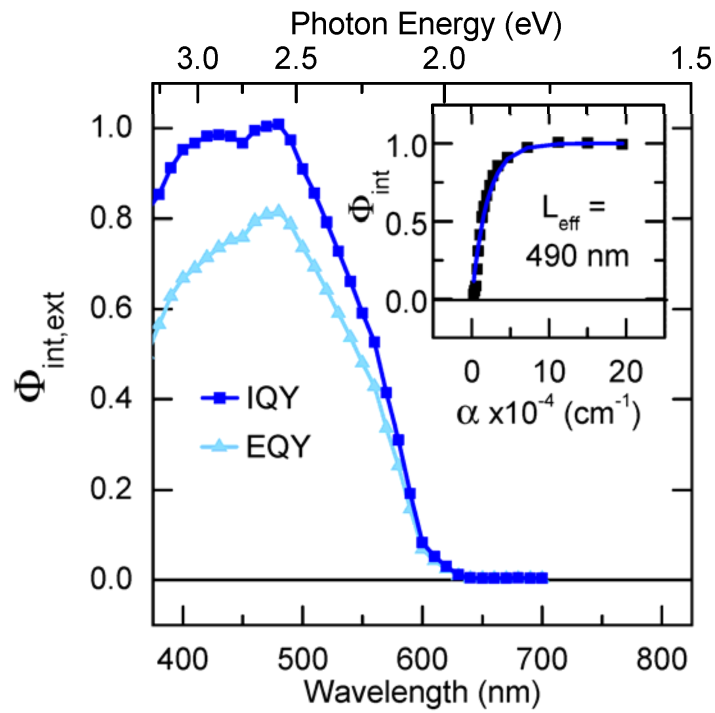

- **Record open circuit potential of > 800 mV in a regenerative photoelectrochemical cell**
- Internal quantum yields ≈ 100% from 400 – 500 nm

C. Xiang, **G. M. Kimball**, R. Grimm, N. S. Lewis. En. & Env. Sci. DOI: 10.1039/c0ee00554a, 2011.

Light absorption and carrier collection

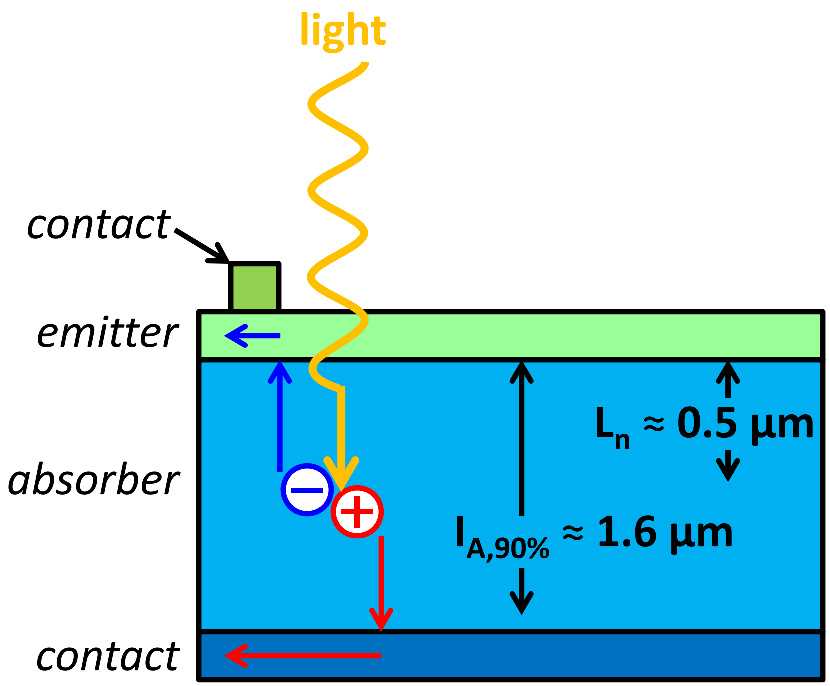

- Absorption length ≈ 1.6 µm for 90% light absorption
- Collection length ≈ 0.5 µm for incomplete carrier collection

Improved collection lengths would enable

> 6% efficient Cu_2O solar cells

C. Xiang, **G. M. Kimball**, R. Grimm, N. S. Lewis. En. & Env. Sci. DOI: 10.1039/c0ee00554a, 2011.

Stability of Cu_2O/liquid junctions

Current-voltage curves

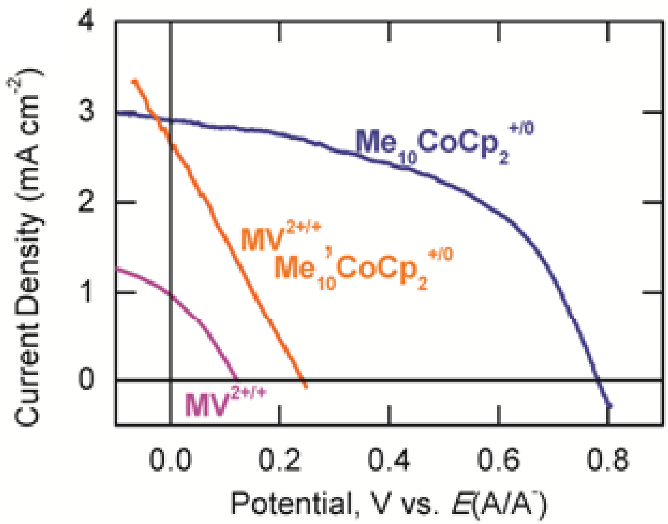

X-ray photoelectron spectroscopy

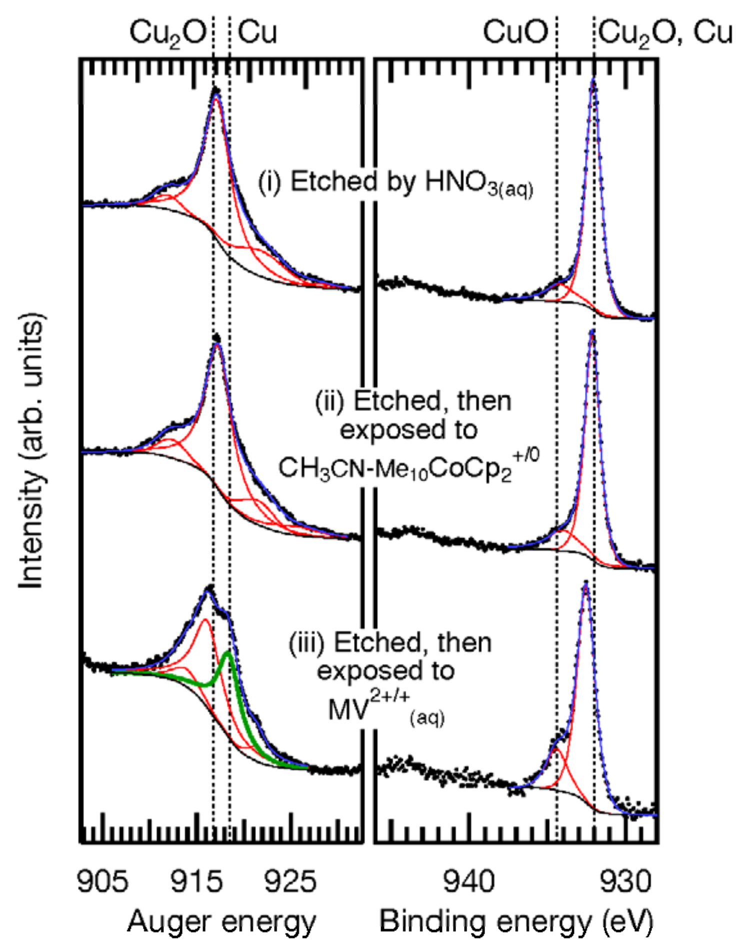

- **Cu_2O is stable in the nonaqueous system**
- Photocorrosion is evident in acid (aq)
- Corroded samples show greatly reduced performance

C. Xiang, **G. M. Kimball**, R. Grimm, N. S. Lewis. En. & Env. Sci. DOI: 10.1039/c0ee00554a, 2011.

Attainable efficiency

All photons collected → J_{sc}^{MAX}

With collection losses → J_{sc}^{IQY}

Collection & absorption losses → J_{sc}^{PEC}

Experimental → J_{sc}^{exp}

Light source	J_{sc}^{MAX} (mA·cm^{-2})	J_{sc}^{IQY} (mA·cm^{-2})	J_{sc}^{PEC} (mA·cm^{-2})	J_{sc}^{exp} (mA·cm^{-2})
AM 1.5	14.1	9.0	5.0	n/a
100 mW·cm^{-2} ELH	13.8	7.2	4.7	3.3
10 mW·cm^{-2} ELH	1.4	0.68	0.44	0.41

Current-voltage curves

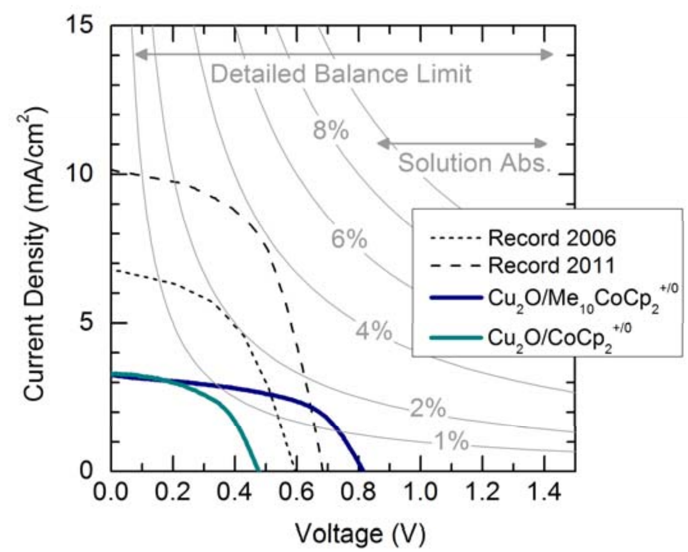

Solution absorption loss ≈ 4 mA·cm^{-2}

Bulk recombination loss ≈ 6 mA·cm^{-2}

C. Xiang, **G. M. Kimball**, R. Grimm, N. S. Lewis. En. & Env. Sci. DOI: 10.1039/c0ee00554a, 2011.

High performance Cu_2O/liquid junctions

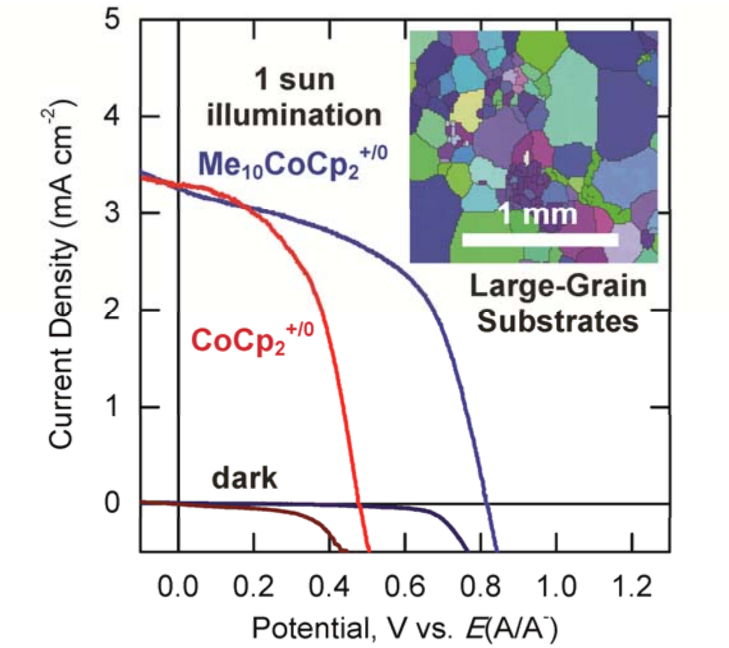

- Achieved open-circuit potential record of 820 mV using a Cu_2O absorber
- Demonstrated internal quantum yields ≈ 100% from 400 – 500 nm illumination
- Showed stable performance of high barrier semiconductor/liquid contacts to Cu_2O

Conclusions

- Prepared high purity substrates of Zn_3P_2 and Cu_2O to investigate their potential for solar energy conversion.
- Revealed $E_{g,indirect}$ = 1.38 eV, $E_{g,direct}$ = 1.50 eV and collection lengths ≥ 7 μm by PL measurements of Zn_3P_2 substrates.
- Examined 4.5% efficient Mg/Zn_3P_2 solar cells to elucidate the passivation reaction of Mg metal with Zn_3P_2 surfaces.
- Demonstrated V_{oc} > 800 mV and internal quantum yields ≈ 100% from 400 − 500 nm for Cu_2O substrates.

Acknowledgements

- Professor Harry Atwater
- Committee: Professors Harry Gray, Mitchio Okomura, Tom Miller, Rick Flagan
- Jeff Bosco, S. Faisal Tajdar, Davis Darvish, Samantha Wilson, Gerald Miller, Michael Deceglie, Michael Kelzenberg, Adele Tamboli, Marina Leite, Vivian Ferry, Krista Langeland, Imogen Pryce, Ryan Briggs, Robert Walters, Seokmin Jeon, Mike Filler
- Alireza Ghaffari, Carol Garland, Steve Rozeveld, Marty DeGroot, Rebekah Feist

Acknowledgements

- Professor Nathan Lewis
- Chengxiang Xiang, Ron Grimm, Astrid Müller, James McKone, Shannon Boettcher, Nick Strandwitz, Liz Santori, Emily Warren, Leslie O'Leary, Steven Maldonado, Matt Traub, David Gleason-Rohrer, David Knapp, Matt Traub
- Brave Undergraduates: Jeanne Peng, Jared Sacco, Charlie Jaramillo, Andrew Gong
- Bruce S. Brunschwig, Jay Winkler, Richard Gerhart, Yunbin Guan, Chi Ma


HOLLYWOOD



Zn_3P_2 and Cu_2O substrates for solar energy conversion

Cornering the market for 'Solar-Grade' Zn_3P_2

Why is annealing critical in Mg/Zn_3P_2 solar cells?

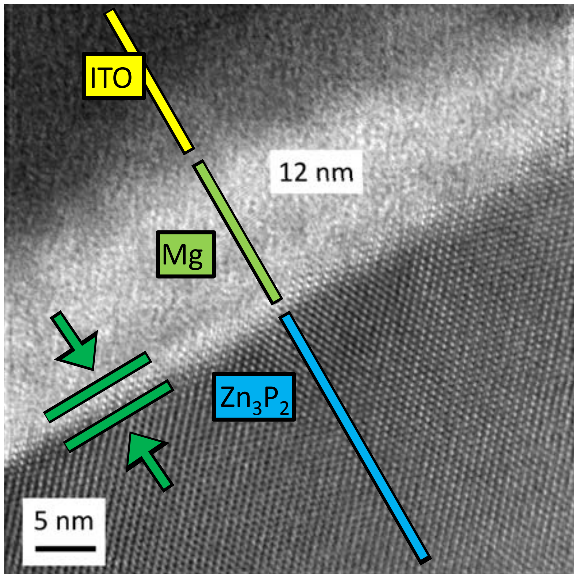

High performance Cu_2O/liquid junctions

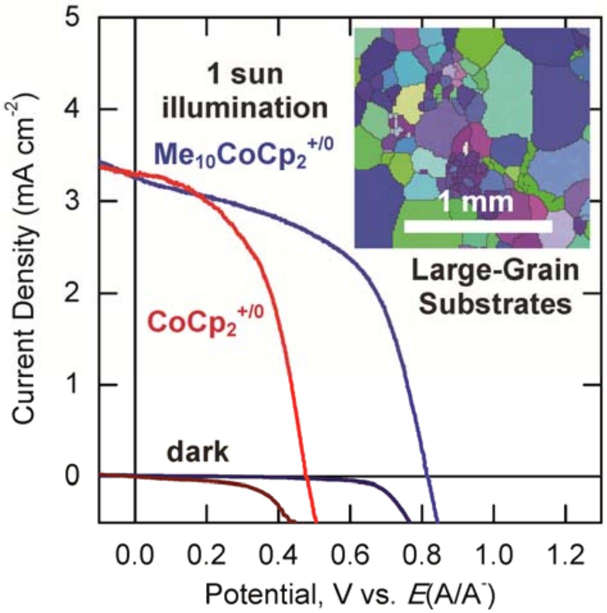

Evaluating Mg-Zn-P Heterojunctions

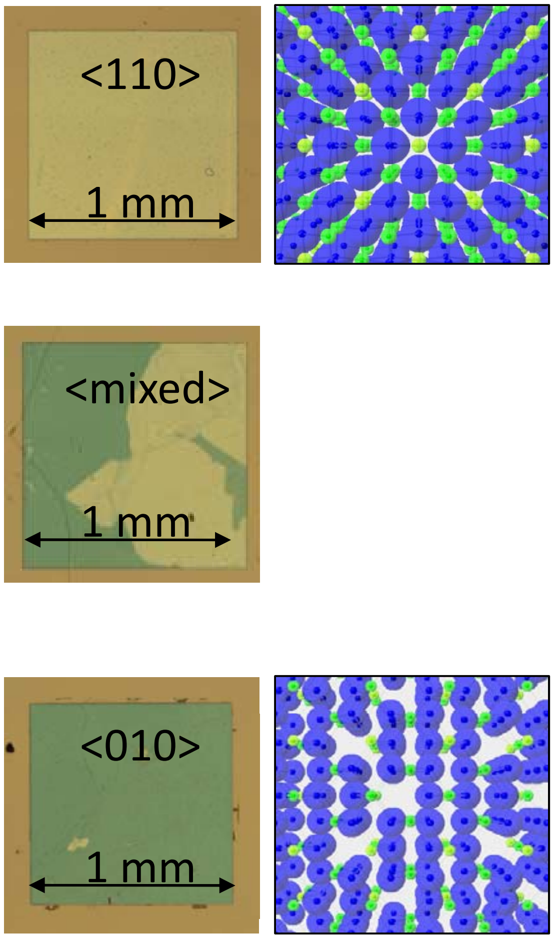

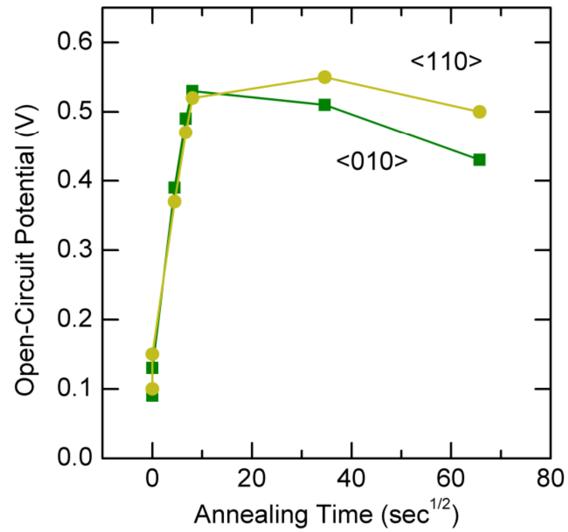

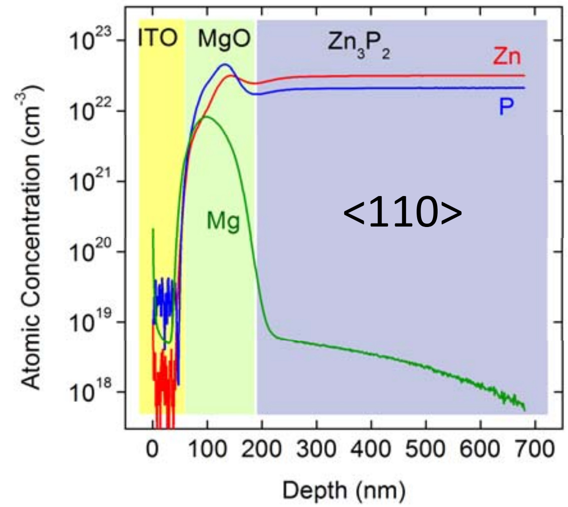

- Mg alloying and doping are orientation-dependent

➢ ***V_{oc} increase is independent of orientation***

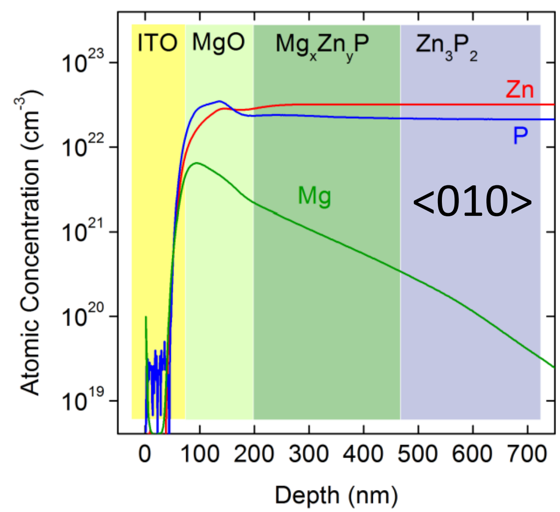

Rough Wafers to Substrates

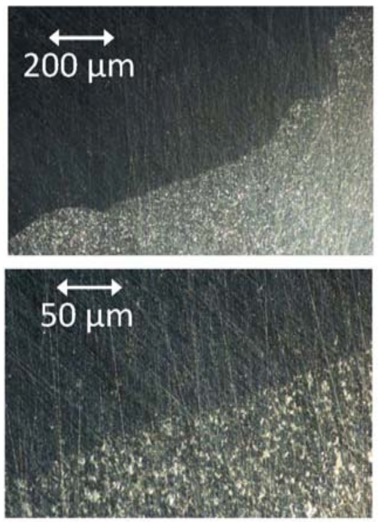

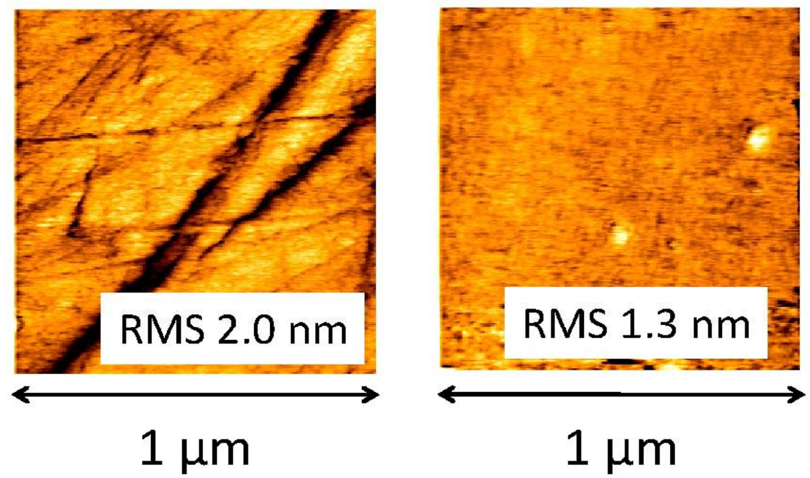

Atomic force microscopy (AFM) images

- Microfracturing for certain grains
- Diamond abrasive pad, diamond slurries and chemical polish

➢ **Specular, 1 – 2 nm RMS roughness Zn_3P_2 substrates**

ITO/Mg/Zn_3P_2 Device Results

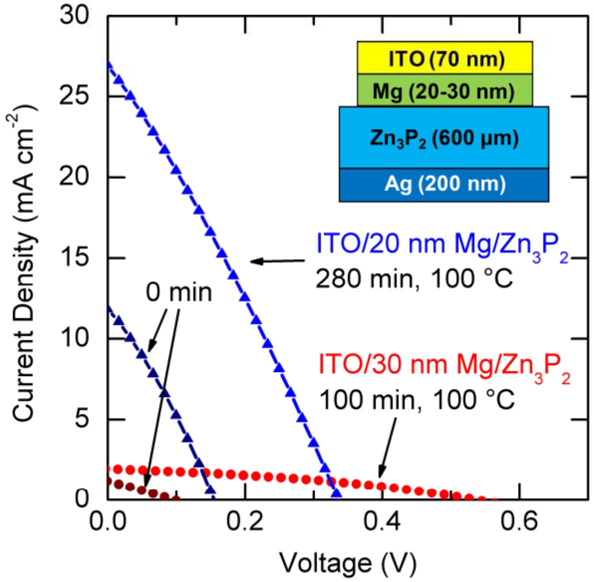

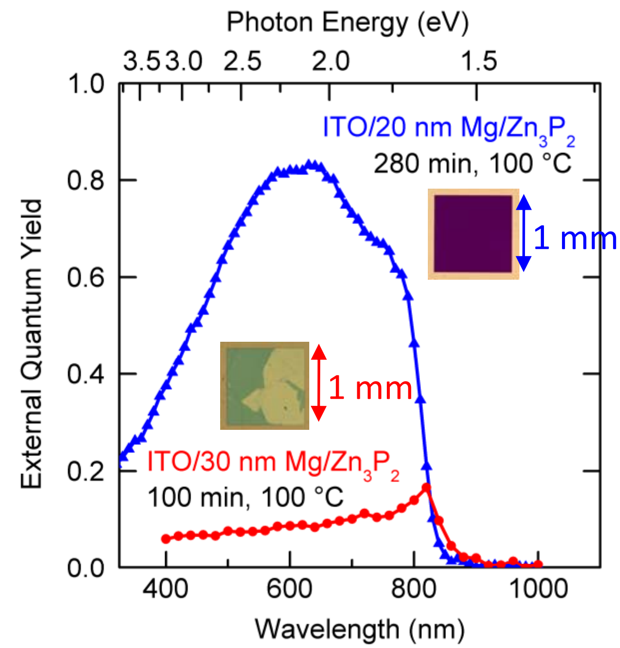

- ITO/Mg/Zn_3P_2 devices show large V_{oc} improvement upon annealing
- Thin Mg layers cause shunting, thick Mg layers increase reflection

➢ **Mg enables high V_{oc} but limits J_{sc} and FF**

G. M. Kimball, N. S. Lewis, H. A. Atwater, *Thirty-seventh IEEE PVSC*, 2011.

Photoelectrochemistry of semiconductors

- Solution potential tunable over a wide energy range
- Control of barrier height for both p- and n-type materials

➢ **Characterize absorber layers without the confounding effects of solid-state junctions**

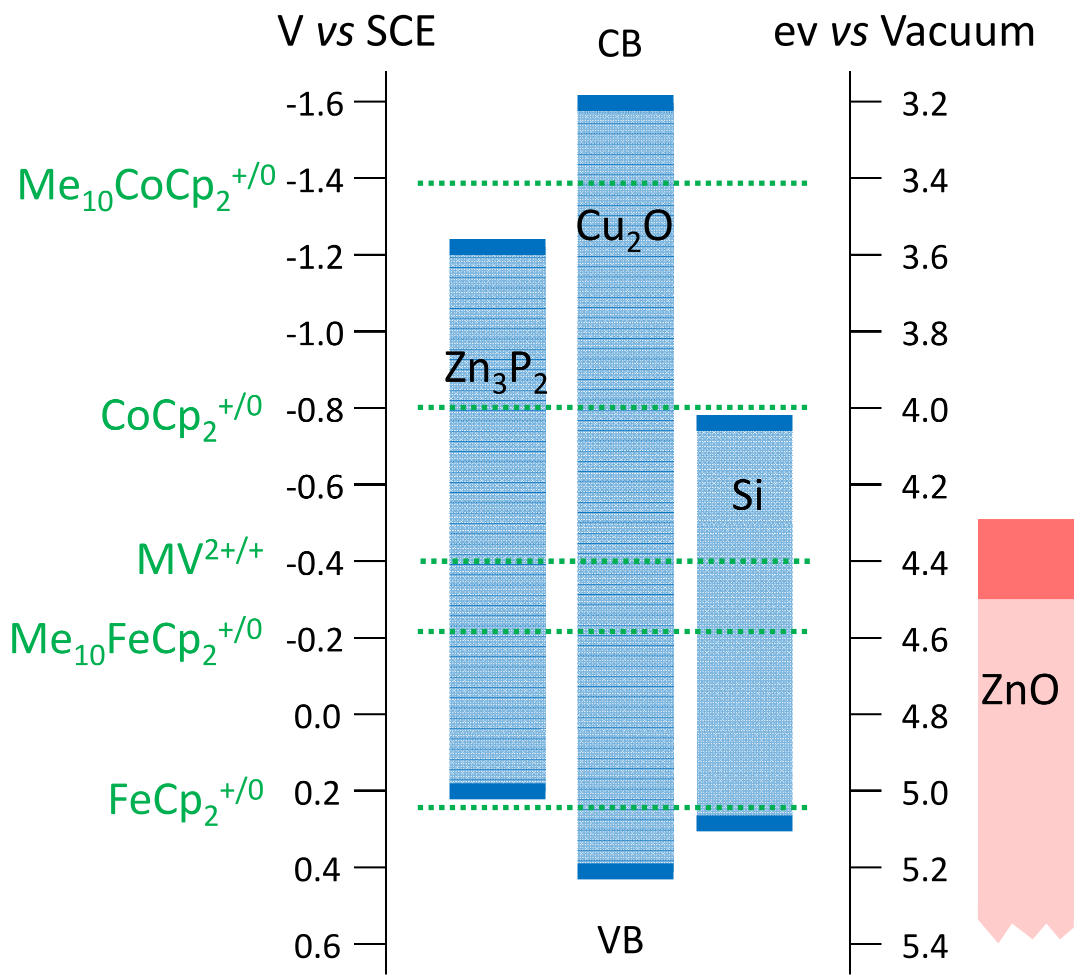

Adapted from N. S. Lewis. Journal of the Electrochemical Society 131.11 :2496-2503. **1984**.

Light intensity dependence behavior

Increased light intensity causes:

- Lower series resistance due to photoconductivity
- Reduced Φ_{ext} due to higher solution absorption

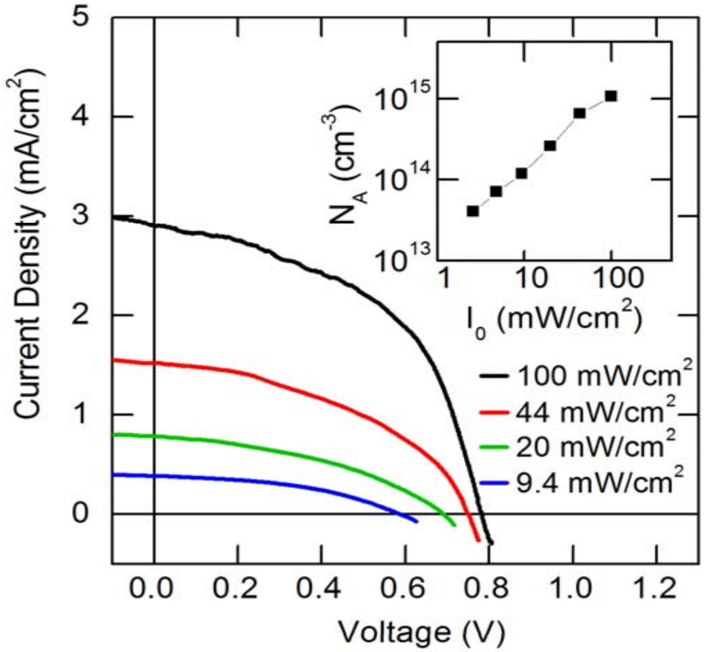

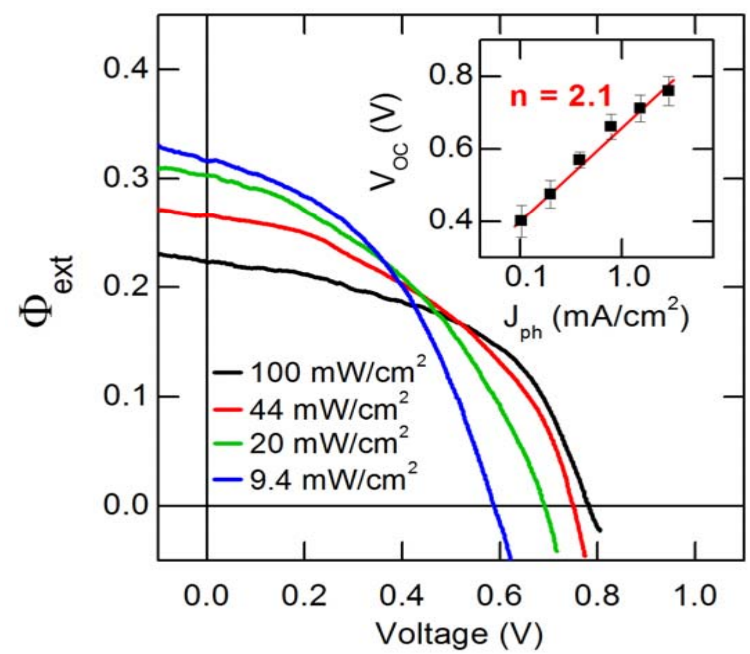

C. Xiang, **G. M. Kimball**, R. Grimm, N. S. Lewis. En. & Env. Sci. DOI: 10.1039/c0ee00554a, 2011.